



**"Application of nano iron in the remediation of Cr-contaminated
soil and its effect on plant growth and soil bacteria"**

**"استخدام النانو حديد في تنظيف التربة الملوثة بعنصر الكروميوم وتأثير ذلك على
نمو النبات وبكتيريا التربة"**

Prepared by

Shireen Tariq Zedany

1125354

Supervisor

Prof. Talal Shahwan

Members of examination committee

Dr. Hani Awad

Prof. Jamil Harb

Date of defense: September 3^{ed} 2015

This Thesis was submitted in partial fulfilment of the requirements for the Master's Degree in Applied Chemistry from the Faculty of Graduate Studies at Birzeit University, Palestine.

**“Application of nano iron in the remediation of Cr-contaminated soil
and its effect on plant growth and soil bacteria”**

“استخدام النانو حديد في تنظيف التربة الملوثة بعنصر الكروميوم وتأثير ذلك على نمو

النبات وبكتيريا التربة”

Prepared by

Shireen Tariq Zedany

1125354

This Thesis was submitted in partial fulfilment of the requirements for the Master’s Degree in Applied Chemistry from the Faculty of Graduate Studies at Birzeit University, Palestine.

Date of defense : September 3^{ed} 2015


Approved, Thesis examination committee :

Prof. Talal Shahwan


(Supervisor)

Dr. Hani Awad


(Member)

Prof. Jamil Harb


(Member)

اهداء

إلى والدي الحبيب السيد طارق خيري عبد الله زيداني

الذي توفي بتاريخ 18-4-2015 ، أخذه القدر ولم يعطيني الفرصة حتى أهديه تخرجي من الماجستير بوجوده بيننا. تمنيت لو أنني أستطيع أن أمنحه لقب "الأستاذ" الذي أحصل عليه مع إنهائي للماجستير بشكل رسمي، ولكنني على الأقل أستطيع أن أمنحه هذا اللقب بشكل رمزي، إلى "الأستاذ طارق زيداني" أبي ومعلمي الأول.

أبي الحبيب، غاب جسده ولكن روحه و تعاليمه التي زرعها داخلي وداخل إخوتي ستعيش معنا الى الأبد، هؤلاء الذين لم تكن الحياة عادلة معهم بحيث لم يعرفوه ولم يعرفو روعة التواجد معه، لقد عرفته بروعة وسمو كونه الأب الذي عشت في كنفه وظله حتى شاء الله وأخذه وتركني من بعده أحاول جبر الكسر الذي خلفه فقده في قلبي وعقلي وكياني وكل وجودي، أحاول كل يوم يا أبي فأجدني منكسرة في غيابك أكثر فأكثر، أسأل الله أن يرحمك وأن يجعل سعبي في كل طريق علم في ميزان أعمالك وحسناتك، وأن يجعل كل ما بذلته في سبيل تربيتي و تعليمي سببا لدخولك الجنة.

Acknowledgments

I would like to express my deep thanks and appreciation to my supervisor Dr. Talal Shahwan for his support and patience throughout the research project, he is a great example to look for academically and personally.

A special thanks to Prof. Jamil Harb for his help in the plant part of this thesis. I also want to thank Dr. Emilia Rappocciolo, the head of the biology and biochemistry department, the lab technician Mr. Rateb Muhamad for their help in the bacteria experiment.

I want to thank the members of the thesis committee Dr. Hani Awad and Prof. Jamil Harb for their time.

I also want to thank all the members of the department of chemistry, lab technicians Mr. Ibrahim shalash and Mr.Asem Mubarak, the secretary of the department Mrs.Ghadeer Tayem, all teaching assistants especially Mrs.Sadieh Abu-SirriAh, Mrs.Asia Shalash, Mrs.Manal Zahran and Miss Raheeq Nasser, for their help and support through the project.

I am thankful to the members of the materials research center at Izmir Institute of Technology in Turkey for their support in XRD, SEM, EDX & BET analysis.

Deep thanks to Prof. Paul Walther and Mrs. Montaha Almasri for thier help in the SEM and TEM analysis that was done in Ulm University in Germany.

Finally, but most importantly, to my family, my mother Mrs. Liana Ajloni for being the strongest, most supporting mother. My brothers Nael and Mohammed, my sisters Loreen, Tasneem and my third sister Sabreen and her angels Tariq and Lolo, thanks for being always by my side, love and care that I am surrounded by will always be my light in the darkness.

To my husband Mr. Mazen Zahran for his love and care, to my unborn baby boy “Ameer”, my closest partner in this journey, thanks for being my joy.

Lastly, to my father Mr. Tariq Zedany, he passed on 18.4.2015, destiny took him and left me alone standing in empty room with nothing to hold on. My father, friend, first teacher and guide in life, my hard work throughout my studying years is dedicated to your soul

knowing it's nothing and not enough to pay back even one billion of your grace on me. May his soul rest in peace and sense my bride and honor.

Table of Contents

1. Introduction.....	1
1.1 Pollution of Cr(VI) in soil and water	1
1.2 Nano iron-general characteristics and applications	4
1.3 Literature review of similar studies	12
1.3.1 Removal of Cr(VI) from water and Soil	12
1.3.2 Effect of nano iron on plant growth	14
1.3.3 Effect of Fe NPs on soil bacteria	18
1.4 Purpose of this study	23
2. Experimental	25
2.1 Preparation of Iron Nanoparticles (nZVI)	25
2.2 Preparation of zeolite-iron nanoparticles	25
2.3 Preparation of GT-Fe NPs	26
2.4 Preparation of Cr(VI) solution	27
2.5 Characterization techniques.....	27
2.5.1 BET surface area analysis.....	31
2.5.2 XRD.....	31

2.5.3 SEM/EDX.....	32
2.5.4 XRF.....	33
2.5.6 HR-TEM	34
2.6 Removal of Cr (VI) from aqueous solution	35
2.6.1 Effect of time.....	35
2.6.2 The effect of initial Cr (VI) concentration	36
2.6.3 Effect of initial pH on the Cr (VI) removal.....	37
2.7 Plant experiments - Effect of Fe NPs on Corn growth	37
2.7.1 The experiment layout.....	37
2.7.2 Preparing soil for planting	41
2.7.3 Planting	41
2.7.4 ICP-OES analysis for soil samples	42
2.8 Effect of Fe NPs on bacteria.....	43
2.8.1 Procedure	46
3. Results & Discussion.....	48
3.1 Characterization of Fe nanomaterials	48
3.1.1 Characterization of nZVI.....	48

3.1.2 Characterization of zeolite-nZVI composite	52
3.1.3 Characterization of “greener” nano iron	54
3.1.4. Characterization of the soil samples	57
3.2 Removal of chromium (VI) from aqueous solution	61
3.2.1 Calibration curve	61
3.2.2 Effect of time.....	62
3.2.3 The effect of initial Cr (VI) concentration	66
3.2.4 Effect of pH of the Cr (VI) solution.....	71
3.3 Effect of Cr(VI) removal from soil mixed with Fe NPs on Corn growth.....	76
3.3.1 Removal of Cr(VI) from soil mixed with Fe NPs	76
3.3.2 Effect of Cr(VI) remediation from soil on Corn growth.....	81
3.4 Effect of iron nanoparticles on bacteria growth	95
3.4.1 <i>Staphylococcus aureus</i>	96
3.4.2 <i>Klebsiella pneumonia</i>	98
3.4.3 <i>Bacillus subtilis</i>	99
3.4.4 <i>Escherichia coli</i>	100

4. Conclusions.....	105
5. References.....	107
APPENDIX A – λ_{\max} . Scan & calibration curve	107
APPENDIX B --- ICP analysis results.....	126

List of Tables

Table 1 Standard reduction potential of Fe ²⁺ and Fe ³⁺ [28].....	9
Table 2 Description of samples characterized at Izmir Institute of Technology.	29
Table 3 Description of samples characterized at Ulm University.....	30
Table 4 Treatments included in the plant experiment	40
Table 5 Samples which were tested in the bacteria experiments	44
Table 6 Types of tested Bacteria.....	44
Table 7 Presentation of the type and order in which chemicals were added to the 24 well plates (each well contains the tested bacteria) .	45
Table 8 XRF analysis results for nZVI	52
Table 9 XRF analysis results for GT-Fe NPs.....	57
Table 10 pH values measured at the beginning and the end of the reaction of Cr(VI) with nZVI	69
Table 11 pH values measured at the beginning and the end of the reaction of Cr(VI) with Z-nZVI.....	70
Table 12 Summary of the quantities of Cr and remediating substances mixed with soil, and the effect of the process on plant progress through two months of planting.....	84
Table 13 Summary of the ICP-OES analysis results for Fe.....	89

Table 14 Summary of the ICP-OES analysis results for Cr.....	90
Table 15 The Δ values obtained from the ICP analysis for Cr(VI) in a descending order	92
Table 16 The Δ values obtained from the ICP-OES analysis for Fe in a descending order	93

List of Figures

Figure 1 Schematic representation of the synthesis of nano-iron materials by borohydride reduction [22].	7
Figure 2 The core-shell model of nZVI and schematic representations of the reaction mechanisms for the removal of several contaminants [27].	8
Figure 3 The plant experiment layout (RCBD).	38
Figure 4 An image of the planting site.	39
Figure 5 Different pictures of the 24 well plates used in the bacteria experiments.	46
Figure 6 SEM image of nZVI aggregates showing its chain like structure.	49
Figure 7 TEM images of nZVI at two different scales (a-200 nm, b-100 nm).	50
Figure 8 XRD pattern of nZVI.	51
Figure 9 SEM image of Z-nZVI (1:1 ratio of zeolite and Fe ²⁺ ions).	53
Figure 10 XRD pattern of Z-nZVI.	54
Figure 11 TEM image of GT-Fe NPs.	55
Figure 12 XRD pattern of GT-Fe NPs.	56
Figure 13 A typical SEM image of soil grains.	58

Figure 14 XRD pattern of a soil sample.....	59
Figure 15 Elemental content of a typical soil sample.....	59
Figure 16 A SEM image of a mixture of soil and GT-Fe NPs.....	60
Figure 17 Variation of Cr(VI) aqueous concentration with time upon contact with nZVI.	63
Figure 18 Variation in the adsorbed amount of Cr(VI) on nZVI with time.	63
Figure 19 Variation of Cr(VI) aqueous concentration with time upon contact with Z-nZVI.	64
Figure 20 Pseudo-first order plot of the removal of Cr(VI) by Z-nZVI	66
Figure 21 The effect of initial Cr(VI) concentration on the removal of Cr(VI) by nZVI.	67
Figure 22 The effect of initial Cr(VI) concentration on the removal of Cr(VI) by Z-nZVI.	68
Figure 23 Effect of initial solution pH on the extent of Cr(VI) removal by nZVI.....	71
Figure 24 Effect of initial solution pH on Cr(VI) removal by Z-nZVI.	72

Figure 25 A schematic representation of (a) monodentate and bidentate ((b) mononuclear and (c) binuclear) inner sphere complexes that Cr(VI) can form with iron hydrous oxide surface [76].	75
Figure 26 EDX mapping of a sample containing soil, Cr(VI) and GT-Fe NPs.	79
Figure 27 XRD pattern of a sample of Soil –GT-Fe NPs loaded with Cr (VI) ions.	80
Figure 28 TEM image of GT-Fe NPs after the reaction with Cr(VI) ions.	80
Figure 29 Some plants that didn't grow.	82
Figure 30 Some plants that grew normally.	82
Figure 31, Figure 32 Corn cobs that appeared in plants with normal growth at the end of the planting cycle.	83
Figure 33 Inhibition of <i>S. aureus</i> bacterial growth in a descending order	97
Figure 34 Inhibition of <i>K. Pneumonia</i> bacterial growth by various solutions in a descending order.	99
Figure 35 Inhibition of <i>B. Subtilis</i> bacterial growth by different solutions in a descending order.	100

Figure 36 Inhibition of *E. coli* bacterial growth in a descending order

..... 101

Abstract

Recently, a huge amount of laboratory-scale research and field tests are being carried out internationally in order to assess the effectiveness of iron nanotechnology in environmental cleanup. Published results have shown that nano iron is an effective tool for remediation of water and soil from various kinds of organic and inorganic pollutants. Together with this, increasing attention is also paid to the impact of nano iron on the biosphere.

In this study, nano iron was applied to remediate soil samples contaminated with chromium. Hexavalent chromium is a well known pollutant in water and soil, particularly in the vicinity of industrial regions. In addition to this, the effect of nano iron on plant growth and soil bacteria was investigated.

This research was conducted in cooperation between Chemistry department and department of Biology and Biochemistry at Birzeit University. Nano iron was synthesized, and its efficiency toward Cr(VI) removal was tested using laboratory scale experiments under various experimental conditions. The assessment of nano iron impact

on plant growth and soil bacteria was realized using the facilities found at the department of Biology and Biochemistry.

The results indicate that both of nZVI and Z-nZVI materials are very effective in Cr(VI) removal, as the percentage removal exceeded 90 percent for most of the studied concentrations. For nZVI, equilibrium of Cr(VI) removal is approached in about one hour of contact between liquid and solid phases. For Z-nZVI, the process was slower and more than four hours were required to attain equilibrium. The data of Z-nZVI obeyed pseudo first order kinetics, with k_1 (rate constant) calculated as $3.4 * 10^{-3} \pm 0.2 * 10^{-3} \text{ min}^{-1}$, and Q_{max} (maximum sorbable amount) found as $24 \pm 1 \text{ mg/g}$.

The removal of Cr(VI) is high over a wide range of pH values, the removal was seen to decrease in the alkaline medium. Generally, the removal of Cr(VI) by Z-nZVI is more pH-dependent than that of nZVI.

The results of EDX mapping analysis showed that the Cr signals are associated with the Fe signals, not with Si, indicating that Cr ions favors binding to iron nanoparticles more than soil.

No negative effect of nZVI and GT-Fe on Corn growth at the lower applied dose (0.1 mg/Kg) on soil fertility and plant nutrition was observed, however, high concentrations of Fe NPs can be harmful to the corn plants.

The results of bacteria tests showed that Cr(VI) solutions have little effect on the tested bacteria types at low concentrations, but detrimental effects at higher concentrations. nZVI (and Cr-nZVI) demonstrated the highest detrimental effect, GT-Fe NPs had less detrimental effect than nZVI. The extent of the effect will depend significantly on the applied concentration.

ملخص

في الآونة الأخيرة، يجري تنفيذ كمية كبيرة من البحوث والاختبارات الميدانية من أجل تقييم فعالية تكنولوجيا النانو الحديد في تنظيف البيئة. وقد أظهرت النتائج التي نشرت أن نانو الحديد هو أداة فعالة لمعالجة المياه والتربة من أنواع مختلفة من الملوثات العضوية وغير العضوية. مع هذا، يولى اهتمام متزايد أيضا لتأثير نانو الحديد على المحيط الحيوي.

في هذه الدراسة، تم استخدام نانو الحديد لتنظيف عينات من التربة الملوثة مع الكروم. الكروم (VI) هو من الملوثات المعروفة في الماء والتربة، وخاصة في المناطق القريبة من المنشآت الصناعية. بالإضافة إلى ذلك، تم دراسة تأثير نانو الحديد على نمو النبات و بكتيريا التربة.

أجريت هذه الدراسة بالتعاون بين قسم الكيمياء وقسم الأحياء والكيمياء الحيوية في جامعة بيرزيت. تم تصنيع نانو الحديد، واختبار كفاءتها نحو إزالة الكروم (VI) باستخدام تجارب على نطاق المختبر في قسم الكيمياء. وأجريت التجارب تحت ظروف مخبرية مختلفة. وقد تم تقييم تأثير نانو الحديد على نمو النبات و بكتيريا التربة باستخدام مرافق وجدت في قسم الأحياء والكيمياء الحيوية.

المنهجية المستخدمة في هذا البحث هي محاولة لتقييم الاستفادة من نانو الحديد واختبارها أيضا ومعرفة إلى أي مدى قد يكون لها آثار سلبية على البيئة المحيطة، إن وجدت، على التربة والنباتات والبكتيريا. ومن المتوقع أن تسهم النتائج في المعارف العالمية حول الفوائد فضلا عن المخاوف بشأن التطبيقات من نانو الحديد في تنظيف البيئة.

1. Introduction

1.1 Pollution of Cr(VI) in soil and water

Chromium, discovered in 1797, took its name from the Greek word 'chroma' which means color, because of the many different colors found in its compounds. This element is the earth's 21st most abundant element, and the sixth most abundant transition metal [1].

The metal content in soil is a sum of metals originating from natural processes and human activities [2]. Natural processes result in heavy metal content derived from parent rocks, while anthropogenic contamination includes agrochemicals, organic amendments, animal manure, mineral fertilizer, sewage sludge, and industrial wastes [3].

Heavy metals are among the most significant soil contaminants, due to their long-term toxicity effects [4] as they are non biodegradable and non thermodegradable [5]. In general, increase in metal content in soils is observed in areas of intense industrial activities [2],[4],[6].

Moreover, effluent slurries with high heavy metal content is a common waste liquid which have been frequently disposed by a variety of industrial processes. It is reported that heavy metal contamination of water sources may last for decades [6].

Heavy metals can accumulate to toxic levels because they are non biodegradable and non thermodegradable [5]. It is well known that heavy metals are essential for living thing at certain levels but that toxic effects appear if the intake exceeds the limit values. Soil and water contaminants can penetrate into the food chain by plants and through direct consumption by animals feeding on them. High doses of heavy metals are known to cause carcinogenic, teratogenic, toxic, or cardiovascular problems. Therefore, metal pollution in areas of agricultural activities forms a great concern [4]. Moreover, the toxicity of heavy metals to organisms can affect the microbiology of the soil ecosystem [7],[8], [9].

Industrial activities that can increase Cr concentration in soils include steel production, leather tanning and corrosion prevention [7]. In addition, soils irrigated by wastewater can accumulate heavy metals such as Cr and can release heavy metals into ground water available for plant uptake [5].

As is known from basic Chemistry, transition metals exist in different oxidation states due to the presence of empty 'd' orbitals in transition metal ions, and thus can form various species in solution [8]. The most

stable oxidation states of Cr in soil and water are Cr(III) and Cr(VI). Each of them exhibit markedly different mobility and toxicity; Cr(VI) is well known to be more toxic and more mobile than Cr(III). In addition to these forms of Cr, other valence states which are unstable and short lived can exist in biological systems [10].

The reduction of Cr(VI) ions is environmentally beneficial because it decreases the threat of these ions to human health [7]. According to World Health Organization (WHO) regulations, the maximum permissible limit of total Cr in drinking water is 50 ppb [8].

The high toxicity of Cr(VI) is results from being both a mutagen and a suspected carcinogen, and being quite soluble in water almost over the entire pH range. In acidic soil, however, Cr(VI) may be adsorbed and reduced to the far less mobile Cr(III) in presence of ferrous iron [11].

Soil quality and content can affect productivity of crops and livestock, environmental quality of natural resources, in addition to health of plants, animals, and humans [12]. In spite of the the useful applications of Cr, the impact of its industry on the local environment is extensive, complicated and not fully quantified [13]. Moreover, the

natural occurrence of Cr ranges from 10 to 50 mg/kg depending on the parental material [10].

Due to its serious hazards, it is necessary to remove Cr(VI) from wastewaters prior to their discharge into the environment. Various remediation technologies such as membrane filtration, electrodialysis, ion exchange and adsorption have been developed and employed so far to remove Cr(VI) from wastewaters. However, each of these methods has its own limitations, which makes it necessary to test and develop new materials and more efficient technologies [14].

1.2 Nanoscale iron; general characteristics and applications

Nanomaterials and nanoparticles can be defined as materials manufactured or produced with at least one dimension under 100 nm size. These materials are known to display novel properties depending on their small size [15].

Engineered nanoparticles (ENPs) term is used to refer to nanoparticles manufactured with novel properties. These materials possess different optical, electrical, magnetic, chemical and mechanical properties from their bulk counterparts. In nanoscale range quantum effects start to predominate and the surface-area-to-volume (SA/V) ratio becomes very large. The increase in SA/V ratio results in increased surface

activity of the material and changes their properties and behaviour [16].

The increased surface activity enhances the tendency of nanomaterials to adsorb, interact and react with other atoms, molecules and complexes to achieve charge stabilization. Such unique properties have been shown as beneficial for a wide range of applications [17].

As a result of size reduction, properties are modified. For example, opaque substances become transparent (copper); stable materials become combustible (aluminum); inert materials become catalysts (platinum); insulators become conductors (silicon); and solids turn into liquids at room temperature (gold) [16].

Iron is the fourth most abundant element in the Earth's crust [18]. Since the introduction of zero-valent iron (ZVI) for water purification in 1990, many contaminants have been successfully removed by reductive transformation [19]. ZVI is a well known remediation agent because of its use in permeable reactive barriers, which are used in the treatment of contaminated soil and groundwater with distinct contaminants such as halogenated hydrocarbons or heavy metals [20]. Nanoscale zero-valent iron (nZVI) technology has been widely investigated for the treatment of environmental pollutants in the last

two decades. The material has the advantage of a large specific surface area and great intrinsic reactivity of surface sites [21]. The effectiveness of the material is due to the small particle size and low standard potential and easiness of preparation. In addition, Fe is known to possess a relatively high recommended safety limit and daily intake requirement, compared with other metals [22]. A typical schematic representation of the preparation method of nZVI is shown in Fig. 1.

It has also been reported that ZVI nanotechnology is cost effective for in situ and ex situ remediation. By virtue of their high surface/volume ratios, nZVI possess enormous amount of energy that brings about a high sequestration capacity and provide a kinetic advantage in the uptake process [23].

One important limitation of nZVI technology is caused by the rapid aggregation/agglomeration of individual iron nanoparticles prepared using traditional methods. The material tends also to react quickly with the surrounding media (e.g. dissolved oxygen or water), resulting in rapid loss in reactivity. Because agglomerated ZVI particles are often in the range of micron scale, they are essentially not transportable or deliverable in soils, and thus, cannot be used for in

situ applications. Several methods have been proposed to solve this problem. One approach is attaching nZVI to a support material [24].

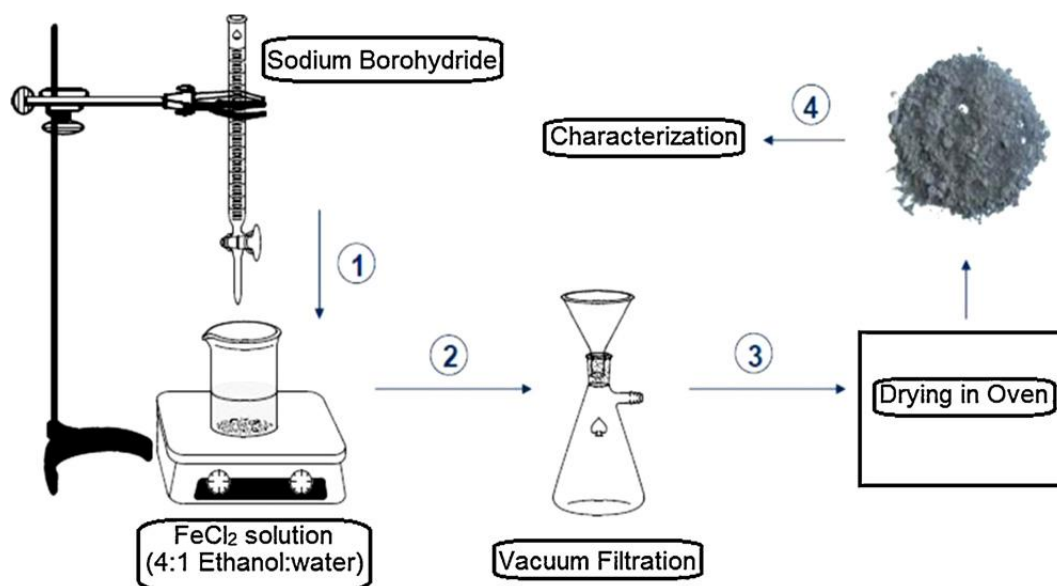


Figure 1 Schematic representation of the synthesis of nano-iron materials by borohydride reduction [22].

During the last few years, ‘green synthesis’ has been presented as a serious alternative for the chemical preparation of iron nanoparticles. It has received considerable attention due to its eco-friendly characteristics. In this method, plant extracts and materials represent an alternative to chemical and physical methods for the synthesis of NPs [25].

Green synthesis has additional advantages because it is easily scaled up for large scale synthesis, and in this method there is no

need to use high energy, temperature, and toxic chemicals. Green synthesis offers better influence, control over crystal growth and their steadiness [26].

Bare nZVI particles are typically less than 100 nm in diameter. In aqueous solutions, all nZVI particles react with water and oxygen to form an outer iron (hydr)oxide layer. As a result, nZVI particles are well known to have a core-shell structure [6], as shown in fig. 2, which proposes conceptually a structural model of nZVI and its reactions with several contaminants [27].

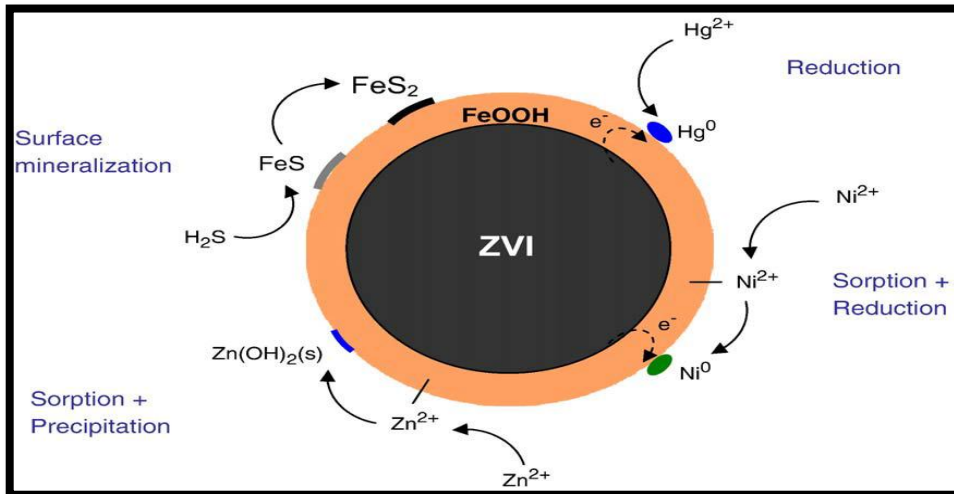


Figure 2 The core-shell model of nZVI and schematic representations of the reaction mechanisms for the removal of several contaminants [27].

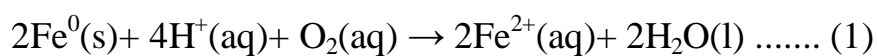
The core forms an electron source that can reduce a wide range of inorganic and organic pollutants, while the shell surface has the ability to adsorb many ions or molecules through physical or chemical sorption. The oxide layer is thought to comprise of mixed Fe(II)/Fe(III) oxides near the interface with Fe⁰ and mostly Fe(III) oxide near the oxide/water interface. This core-shell structure has important implications for the chemical properties of nZVI [27].

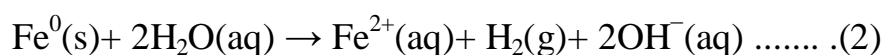
Metallic or zero-valent iron (Fe⁰) is considered a moderate reducing reagent. Table 1 gives the standard reduction potential of Fe²⁺ and Fe³⁺ in comparison with other ions [28].

Table 1 Standard reduction potential of Fe²⁺ and Fe³⁺ [28]

Cathode (reduction) half reaction	Standard potential E ⁰ (volts)
Fe ²⁺ (aq) + 2e ⁻ -> Fe(s)	-0.41
Fe ³⁺ (aq) + 3e ⁻ -> Fe(s)	-0.04

Metallic iron can react with dissolved oxygen (DO) and to some extent with water according to the reactions [29]:



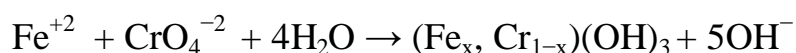


The above equations are the classical electrochemical/ corrosion reactions by which iron is oxidized upon exposure to oxygen and water [29].

To date, nZVI has been developed and used to degrade a wide range of organic and inorganic soil and water contaminants, including halogenated organic compounds, polycyclic aromatic hydrocarbons (PAHs), pesticides, and heavy metals [30].

In recent years nZVI has been developed and demonstrated to be an effective reductant for the immobilization of Cr(VI) in water and soils [31]. Concerning the removal of Cr and its relevant species, studies carried out so far showed the potential of application of iron nanoparticles in the removal of Cr from groundwater, wastewater, and soil [32].

The previous results suggested that Cr(VI) could be rapidly reduced and immobilized by nanoscale iron-based particles without secondary pollution induced by toxic ions [33]. Metals with standard redox potential (E^0) are much more positive than Fe^0 (e.g., Cr) are preferentially removed by reduction and precipitation [6]. The suggested reaction for Cr reduction and immobilisation is:



in which the toxic or carcinogenic hexavalent form of Cr is reduced to the less toxic Cr(III) form, which readily precipitates as $\text{Cr}(\text{OH})_3$ or as the solid solution $\text{Fe}_x\text{Cr}_{1-x}(\text{OH})_3$ [18], (a solid solution is a solid-state solution of one or more solutes in a solvent. Such a mixture is considered a solution rather than a compound, when the crystal structure of the solvent remains unchanged by addition of the solutes, and when the mixture remains in a single homogeneous phase).

In addition to the redox mechanism, some Cr(VI) can be directly adsorbed on the hydr(oxide) shell of nZVI [6].

In the context of soil remediation, trace elements cannot be destroyed like organic contaminants, they can only be relocated. To decrease contaminant bioavailability and mobility, various strategies have been used [34]. The *in-situ* chemical reduction of Cr(VI) by nZVI represents a potentially more effective, lower cost alternative to other remediation techniques such as pump and treat, permeable reactive barriers (PRB) and natural attenuation via bio- and phytoremediation [24]. Stabilization of contaminated soil is a remediation technique that reduces the mobile fraction of trace elements, which could contaminate groundwater or be taken up by soil organisms [35].

1.3 Literature review of similar studies

1.3.1 Removal of Cr(VI) from water and Soil

This section summarizes the findings of previous studies about the applications of Fe NPs and its composite materials in the removal of Cr(VI) ions.

The application of Fe NPs and its composite materials in the removal of Cr(VI) was examined in a number of studies. The reduction and precipitation of Cr(VI) by nZVI was reported to be rapid with a removal capacity ranging from 180 to 50 mg Cr/g nZVI in the pH range of 4 to 8 [36]. In another study effective removal of Cr(VI) by nZVI was reported, and the reaction products were composed of iron oxides, Cr-Fe (oxy)hydroxide and/or the unreacted Fe⁰ [37].

Various materials were used as supports of Fe NPs to assess the removal capacity of Cr(VI) ions. Silica fume-supported Fe⁰ NPs was reported to be reactive in remediation of Cr(VI), and its removal ability was higher than unsupported Fe⁰ under the studied conditions [24]. In another study, nZVI loaded on epichlorohydrin/chitosan beads was reported to be an effective and promising remediation material to remove Cr(VI) from wastewater, and the rate of reaction was a first

order [17]. nZVI supported on a pillared bentonite (Al-bent) was reported to yield almost a complete removal of Cr(VI) ions after 120 min of contact [38]. Bentonite was proven to be an effective dispersant and stabilizer of nZVI, and thus was superior to nZVI in removing Cr(VI) from aqueous solution. Kinetics studies demonstrated that the reduction of Cr(VI) by B-nZVI followed a pseudo-first-order model with almost a complete removal [39]. In another study, nZVI-Fe₃O₄ composites were used in Cr(VI) removal, and the reaction was reported to be more efficient when the temperature increased from 10 °C to 40 °C [40].

The application of Fe NPs was also investigated for the removal of Cr(VI) from soil. For this purpose a new class of sodium carboxy methyl cellulose (CMC)-stabilized nZVI was tested for the in situ remediation of Cr(VI) contaminated soils. The results for the removal of aqueous-bound Cr(VI) indicated that the reduction efficiency was proportional to the CMC-nZVI dosage and inversely related to the initial Cr(VI) concentration, with slightly better performance for acidic or neutral soil remediation [41]. In another study, contaminated soil was stabilized with 1% iron grit. This treatment decreased Cr concentrations in leachates (by 98%), in soil pore water (by 99%) and

in plant shoots (by 84%) [35]. A comparative column study was conducted for the treatment of Cr(VI)-contaminated soil at a Cr plating facility using two agents: calcium polysulfide and Fe NPs stabilized with a polyphenol rich green tea extract. It was concluded from this study that CPS has more favorable properties as injectable reductant for Cr(VI) treatment in soils compared to GT-nZVI [42].

In further applications, stabilized nZVI was applied in the remediation of a simulated Cr(VI)-polluted river. The results showed that the remediation effectiveness was improved with the increasing nZVI dose, decreasing initial concentration of pollution source and water flow rate [43]. In a different work, nZVI was used to reduce Cr(VI) content in Chromite ore processing residue (COPR). The results implied that remediation approaches using nZVI to immobilize Cr(VI) in COPR is successful with sufficient water content to facilitate electron transfer between Cr(VI) and nZVI [31].

1.3.2 Effect of nano iron on plant growth

Iron is one of the essential elements for plant growth and plays an important role in the photosynthetic reactions. Iron activates several enzymes and contributes in RNA synthesis and improves the

performance of photosystems [44]. An important parameter that contributes to this is the existence of two stable, inter-convertible forms of this metal, which take part in fundamental processes involving electron transfer reactions, including respiration and photosynthesis [45].

Plants are an essential base component of all ecosystems and play a critical role in the fate and transport of engineered nanoparticles in the environment through plant uptake and bioaccumulation [46].

The major factors affecting uptake of minerals by plants include soil factors and plant factors. With respect to soil factors, the availability of trace elements as nutrients depends on several parameters, such as lithosphere (base-rock), soil age, soil type and the covering flora. In general, heavy metals can accumulate in higher amounts in the sorption complex of soils rich with organic matter. But the release those metals to soil solution is much slower than in mineral soils due to high affinity of soil organic compounds to heavy metals. Thus, the availability of nutrient metals to plants is controlled also by soil pH, type of mineral colloids and other important factors, like microbial activity, redox potential and aeration [47].

With respect to plant factors, almost all heavy metals can be taken up by plants in two ways, which are mostly concentration-dependent; i) Non-metabolic uptake - by energy independent mechanisms, in which solutes can diffuse down the concentration gradient with the aid of membrane carriers or even aqueous pores. ii) Metabolic uptake - by energy dependent mechanisms. Here, active uptake is involved in taking up ions against their concentration gradient [47].

One of the important consequences of the large increase in the utilization of manufactured nanomaterials is the concern that the release of these materials into the environment may pose a serious threat for the environment [48].

Engineered nanoparticles (ENPs) closely interact with their surrounding environment including plants, and the uptake and accumulation in plant biomass will greatly affect the fate and transport of ENPs in the environment. ENPs could also adhere to plant roots and exert physical or chemical toxicity on plants [46].

Some studies showed that nanoparticles can be beneficial to plants (seedling growth and development) or non-beneficial (to prevent root growth) [44]. However, most studies with ENPs indicated certain degree of phytotoxicity, especially at high concentrations [46]. Other

researchers reported that nZVI particles do not have a significant negative effect on indigenous microbial communities or certain plant species over a long period [49]. It is reported that, for most nanoparticles, relatively high concentrations are needed to cause observable toxicity on plants and that the toxicity threshold is species dependent [50].

The inhibition of plant growth may not be derived directly from chemical phytotoxicity of nanoparticles. Instead, toxicity may result from the physical interactions between nanoparticles and plant cell transport pathways i.e. by inhibiting apoplastic trafficking by blockage of the intercellular spaces in the cell wall or cell wall pores, or the symplastic connections between cells through blockage of the nano-sized plasmodesmata. [46].

It was reported that nZVI at the concentrations used in field conditions could lead to phytotoxic effects on plants and that the extent of toxicity is dependent upon plant species. The result indicated that large scale introduction of nZVI to the environment could lead to serious environmental consequences and thus the environmental impact of such application warrants further attention [51].

The phytotoxicity of nZVI could be explained by several mechanisms. The formation of black coating on the root surface could effectively block the root membrane pores and interfere with the water and nutrient uptake process. Moreover, under reduced conditions, ferrous iron (Fe^{2+}) which is a by-product of iron oxidation, could be further oxidized to its less soluble form of ferric iron (Fe^{3+}) by the oxidative agents released from plant roots and as a result form a cover of an insoluble Fe^{3+} compound on the root surface [51].

Furthermore, the introduction of nZVI could shift the redox condition in the local environment and affect the oxygen release rate of plant roots [51].

1.3.3 Effect of Fe NPs on soil bacteria

Microorganisms exposed to various metal ions in their environment can interact with them. This can be beneficial or detrimental depending on the chemical/ physical nature and oxidation state of the metal ion. Like other heavy metals, chromium can induce multiple toxic effects on tissues and it may affect immune response to bacterial pathogen. Chromium is a unique transition metal ion, which has been

established to be biologically significant at all the levels of living organisms [52].

High concentration of iron is extremely toxic and may enhance bactericide effects of antimicrobial agent or noxious substances, Fe (III) as well as Fe (II) has an inhibitory effect. It is also revealed that other trace elements such as chromium are toxic and could interact with iron metabolism in bacteria. The toxic effects of the trace elements could partially be removed in combination with other elements [52].

Microbes in soil have important impacts on soil and plant. They play significant roles in recycling plant nutrients, maintenance of soil structure, detoxification of noxious chemicals, and the control of plant pests and plant alterations. Being in intimate contact with the soil's environment, soil microorganisms are very sensitive to any ecosystem perturbation, and are therefore considered to be the best indicators of soil pollution [53].

On the other hand, heavy metals exhibit toxic effects on soil biota, and can affect key microbial processes and decrease the number and activity of soil microorganisms [9]. In situ treatment of heavy metal pollution might be expected to affect the plants and the

microorganisms in soil. Microbial toxicity has been reported for metal NPs, like elemental Ag, Au, Fe; oxides of Ti, Fe, Co–Zn–Fe etc [54]. However, other reports on the relative toxicities of heavy metals and metal oxide NPs are contradictory [16].

So far little information is available about the effect of ENPs on the soil microbial community. It is believed that ENPs may have an impact on soil microorganisms via four ways; (1) a direct effect (toxicity), (2) changes in the bioavailability of toxins or nutrients, (3) indirect effects resulting from their interaction with natural organic compounds, and (4) interaction with toxic organic compounds which would amplify or alleviate their toxicity [16].

Many of the reactions involving Fe in soils, sediments, and groundwater are microbially-mediated, with Fe(III) acting as the dominant electron acceptor for microbial respiration in many subsurface environments [18].

Generally, elemental iron itself, such as zero-valent iron, has no known toxic effect, and is one of the most common metals on earth [49]. However, the generated Fe^{2+} ions from the reaction between nZVI and H_2O could be toxic to microorganism, and it is necessary to

investigate the potential releasing toxic ions from nZVI or its reaction product [55].

Recently, however, a study showed that bacterial exposure to nZVI would cause significant disruption to the cell membranes and leakage of the intracellular content [49]. In another study, nZVI was proved to be non-toxic to microorganism in a long term, and the issue of safety caused by anthropogenic injection of nZVI could be avoided [43]. Another work stated that nZVI might be toxic to indigenous bacteria and hinder their participation in the cleanup process [56]. Several studies have shown that iron nanoparticles are cytotoxic to pure cultures of bacteria, such as *Escherichia coli* [57] and *Bacillus subtilis* var. *Niger* [58].

Like in the case of plants, toxicity mechanisms on bacteria and microorganisms have not yet been completely elucidated for most ENPs. However, it is believed that possible mechanisms include disruption of membranes or membrane potential, oxidation of proteins, genotoxicity, interruption of energy transduction, formation of reactive oxygen species, and release of toxic constituents [16]. Nanoecotoxicology is an emerging discipline with useful progress mainly with regards to toxicity occurring in plant, fish and

invertebrate species. However, important gaps remain in the knowledge of other ecological receptors, such as soil microbial communities [34]. Ethical and environmental concern for organisms living in soil and surface water has led to questions of possible negative secondary effects which have scarcely been addressed so far [59]. This issue remains an important one that needs further research and consideration.

Staphylococcus aureus is a type of bacteria. It stains Gram positive and is round shaped. It is called Staphylococcus as it is found in grape-like (staphylo-) clusters. *Staphylococcus* is one of the five most common causes of infections after injury or surgery.[60] *Staphylococcus aureus* can be found in a wide variety of locations such as soil, human skin, and public places like hospitals and prisons [61].

Klebsiella pneumoniae is a Gram-negative, rod-shaped bacterium. It naturally occurs in soil, and can fix nitrogen in anaerobic conditions. *K. pneumoniae* has been demonstrated to increase crop yields in agricultural conditions [62].

Bacillus subtilis cells are rod-shaped, Gram-positive bacteria that are naturally found in soil and vegetation [63],[64].

Escherichia coli (*E. coli*) bacteria normally live in the intestines of people and animals. Most *E. coli* are harmless and actually are an important part of a healthy human intestinal tract.[65] *Escherichia coli* is a gram-negative, anaerobic, rod-shaped bacterium [66].

1.4 Purpose of this study

In this study, Fe NPs were prepared using two methods; nano-zero-valent iron (nZVI) prepared by sodium borohydride reduction method, and ‘greener’ iron nanoparticles (GT-Fe) prepared by using green tea extract as a reducing and stabilizing agent. In addition, nZVI supported on zeolite was also used.

The materials were characterized using Scanning Electron Microscopy (SEM) and Transmission Electron Microscopy (TEM) to investigate and compare their nanoscale morphology. X-Ray powder Diffraction (XRD) was used to determine the mineralogical structure of the materials. Energy Dispersive X-Ray Analysis (EDX) and X-ray Fluorescence (XRF) were employed to determine the quantitative elemental surface composition. BET technique was used to determine the specific areas of the prepared materials.

The prepared materials were then used in the removal of Cr(VI) from aqueous solution. The removal capacities were investigated under various contact times, initial Cr(VI) concentrations, and pH values to determine and compare the removal kinetics and extent of removal. Cr(VI) concentration was determined using UV-visible spectrophotometry.

The prepared materials were then used to remove Cr(VI) from soil. The effect of the remediation process on plant growth was investigated with Corn used as a model plant. Soil samples were analyzed at the beginning and after two months of planting with ICP-OES to determine the Cr and Fe concentration in soil.

Furthermore, the effect of the prepared materials on bacteria growth was investigated. For this purpose, four different types of bacteria that are usually available in soil were tested, two of them are gram positive (*Staphylococcus aureus* and *Bacillus subtilis*) the other two are gram negative (*Klebsiella pneumonia* and *Escherichia coli*).

2. Experimental

2.1 Preparation of Iron Nanoparticles (nZVI)

The procedure applied for this purpose was also reported in earlier studies [1,2]. It relies on the liquid phase reduction method utilizing borohydride as a reducing agent of iron ions. In order to prepare nZVI, 5.34 g sample of ferrous chloride ($\text{FeCl}_2 \cdot 4\text{H}_2\text{O}$) was dissolved in 25.0 ml solution of absolute ethanol and water (4:1 v/v). A 2.54 g sample of sodium borohydride (NaBH_4) was separately dissolved in 70.0 mL water, it was then added dropwise onto the Fe^{2+} solution kept under well stirring.

After the addition of all the borohydride solution, the iron sample was separated using suction filtration, and subsequently washed three times with absolute ethanol (this is an important step to avoid oxidation of Fe^0). The nZVI powder was then dried for about 6 hours in the oven (LDO 030E,060E,100E) which was kept at 90 °C.

2.2 Preparation of zeolite-iron nanoparticles

The composite of iron nanoparticles supported on zeolite (Z-nZVI) was prepared using the borohydride reduction method in accordance with the procedure reported earlier [1,2]. Z-nZVI was prepared in 1:1

zeolite / Fe^{2+} mass ratio by dissolving 5.34 g of $\text{FeCl}_2 \cdot 4\text{H}_2\text{O}$ (Aldrich 22029-9) in 25.0 mL (4:1 ethanol/water) solution. Subsequently, 1.5 g of zeolite (obtained from Inamarble Company) was added to the solution and mixed on a magnetic stirrer for 15 min. NaBH_4 (Merck 8.06373.0025) solution was prepared separately by dissolving 2.54 g in 70.0 mL deionized water, then it was added using a burette to the iron–zeolite solution under continuous stirring. Following the borohydride addition, the solution was kept under continuous stirring for another 15 min then filtered under suction and washed 3 times with absolute ethanol. Finally, the Z-nZVI composite was dried in the oven at 90°C for 6 h.

2.3 Preparation of GT-Fe NPs

The samples were prepared in accordance with a procedure reported earlier [69]. For this purpose, green tea extract was obtained by heating 60.0 g L^{-1} green tea (Alwald Brand) until boiling. After settling for 1.0 h, the extract was vacuum-filtered. Separately, a solution of 0.10 M $\text{FeCl}_2 \cdot 4\text{H}_2\text{O}$ was prepared by adding 19.9 g of solid $\text{FeCl}_2 \cdot 4\text{H}_2\text{O}$ (Aldrich 22029-9) in 1.0 L of deionized water. Subsequently, 0.10 M $\text{FeCl}_2 \cdot 4\text{H}_2\text{O}$ solution was added to 60.0 g L^{-1} green tea in 2:3 volume ratio. Following this, 1.0 M NaOH solution

was added until the pH reached 6.0 and the formation of GT-Fe NPs was marked by the appearance of an intense black precipitate.

The solid phase was separated in two step; first by evaporating water from the iron solution on a hot plate (Freed Electric), and then by drying it overnight in a fume hood.

2.4 Preparation of hexavalent chromium Cr(VI) solution

A 500 mg/L stock Cr(VI) solution was prepared by dissolving 141.4 mg of potassium dichromate ($K_2Cr_2O_7$, Aldrich 20924-4) in 100 ml distilled water. The solution was used to prepare other solutions at concentrations of 0.1, 0.2, 0.4, 0.6, 0.8, 1.0, 10.0, 20.0, 30.0 mg/L. The UV-visible absorbance readings of these solutions were recorded (at $\lambda_{max} = 350$ nm) and a calibration curve was constructed. The instrument used for the UV-Vis. measurements was a Varian Cary 50 Spectrophotometer. The scanned curve containing λ_{max} of chromium solution and the calibration curve are provided in appendix A.

2.5 Characterization techniques

Appropriate physical and chemical characterization of natural and manufactured NMs is fundamental to determine their intrinsic properties [70].

The solid samples used in this study were characterized using Scanning Electron Microscopy/Energy Dispersive X-ray Analysis (SEM/EDX), powder X-ray Diffraction (XRD), X-ray Fluorescence (XRF), Surface area analysis (BET-N₂), and Fourier Transform-Infrared Spectroscopy (FT-IR). All the soil samples were taken at the beginning of the planting experiments. All the above instruments, except the FTIR, are located at Izmir Institute of Technology in Turkey. The samples characterized using these techniques are given in Table 2.

Table 2 Description of samples characterized at Izmir Institute of Technology.

#	Sample Description	Symbol
1	Zero valent iron NPs	nZVI
2	Zeolite supported iron NPs	Z-nZVI
3	Greener iron NPs	GT-Fe
4	Soil only	Soil
5	Soil containing Chromium	Soil + Cr
6	Mixture of Soil and Greener iron NPs	Soil + GT-Fe
7	Mixture of Soil, Chromium, and Greener iron NPs	Soil+Cr+GT-Fe

In addition, the samples given in Table 3 were characterized with SEM & TEM instruments located at Ulm University in Germany.

Table 3 Description of samples characterized at Ulm University

#	Sample Description	Symbol
1	Soil only	Soil
2	Greener iron NPs	GT-Fe
3	Zero valent iron NPs	nZVI
4	Soil after the reaction with Cr(VI)	Soil*
5	Mixture of Soil and Greener iron NPs after the reaction with Cr(VI)	Soil + GT-Fe *
6	Greener iron NPs after the reaction with Cr(VI), initial pH = 2	GT-Fe – 2
7	Greener iron NPs after the reaction with Cr(VI), initial pH = 4	GT-Fe – 4

Sample 4 in Table 3 was prepared by mixing 100-ml of 500 mg/L Cr (VI) solution with 15.0 g soil. To prepare sample 5, 5.0 g of GT-Fe were added to the Cr(VI) solution with the 15.0 g soil. For samples 6 and 7, 5.0 g of GT-Fe were added to the Cr (VI) solution, and the pH of the Cr (VI) solution was adjusted with 0.1 M HCl and 0.1 M NaOH at pH=2 for sample 6, and pH=4 for sample 7. All samples were then

left in contact for 48 hrs, then filtered and dried in the oven at 90°C for 3 hrs.

2.5.1 BET surface area analysis

Brunauer–Emmett–Teller (BET) theory explains the physical adsorption of gas molecules on a solid surface and serves as the basis for an important analysis technique for the measurement of the specific surface area of a material [71].

Samples 4, 5, 6 and 7 given in Table 2 were analyzed for their surface areas using the BET-N₂ method. For this purpose, a Micromeritics Gemini V (Georgia, USA) type instrument was employed.

2.5.2 XRD

X-ray diffraction (XRD) relies on the dual wave/particle nature of X-rays to obtain information about the structure of crystalline materials.

A primary use of the technique is the identification and characterization of compounds based on their diffraction patterns [72].

XRD analysis was performed using a Philips X'Pert Pro (Almelo, Netherlands) instrument. The source consisted of Cu K_α radiation

($\lambda=1.54 \text{ \AA}$), and each of the analyzed samples was scanned within the 2θ range of 20-80.

Samples 1 through 7 in Table 2 were all characterized with XRD. The obtained data were processed and analyzed using MS Origin Pro. 9 software.

2.5.3 SEM/EDX

The scanning electron microscope (SEM) employs a focused beam of high-energy electrons to generate signals from the surface of solid specimens, in order to reveal information about the sample including external morphology (texture), chemical composition, and crystalline structure and orientation of materials making up the sample [73].

Energy Dispersive X-Ray Analysis (EDX), is an x-ray technique used to identify the elemental composition of materials. EDX systems are attachments to SEM or TEM instruments (in this study EDX is attachment to the SEM instrument). Elemental mapping of a sample and image analysis are also possible [74].

SEM/EDX analysis was obtained using a FEI Quanta 250 FEG (Oregon, USA) type instrument. The solid samples were first

sprinkled onto adhesive metallic disks, and the images of the sample surfaces were recorded at different magnifications.

This analysis was performed for all samples in Table 2. In addition to the above, elemental and mapping EDX analysis was performed using the same instrument for sample 7 (Table 2) at randomly selected areas to determine the atomic distribution of elements on the surface of the solids.

SEM analysis was performed for all samples given in Table 3. The instrument used in analysis was a Hitachi, S-5200 field-emission scanning electron microscope, Hitachi, Tokyo, Japan. The accelerating voltage was 10 kV, and the images were taken with the secondary electron detector.

2.5.4 XRF

X-ray fluorescence (XRF) is an elemental analysis technique with broad application in science and industry. XRF is based on the principle that individual atoms, when excited by an external energy source, emit x-ray photons of a characteristic energy or wavelength. By counting the number of photons of each energy emitted from a sample, the elements present may be identified and quantified [75].

XRF measurements were performed using a METEC spectro IQ II (Kleve, Germany) type instrument. The Samples were pulverized in a mortar and thoroughly milled powder was stored in plastic mini centrifuge tubes. During the analysis, the samples were mounted on glass slides and placed in the XRF sample holder.

This analysis was performed for all samples in Table 2.

2.5.6 HR-TEM

High resolution transmission electron microscopy (HR-TEM) is a valuable tool which allows the corroboration of structure, morphology, as well as diffraction data for nanomaterials [76].

The instrument type was a Jeol-1400 transmission electron microscope, Jeol, Tokyo, Japan. The accelerating voltage was 120 kV, bright field signal. A very small amount of each sample was taken in a plastic tube and mixed with a resin. Samples were then centrifuged and left to dry for two days.

A cross section to ultra thin layers was prepared under the microscope. Then the thin section was placed on a copper grid and fixed on the device holder, the parameters were finally adjusted to obtain clear images. This analysis was done for all samples in Table 3.

2.6 Removal of Cr (VI) from aqueous solution

All the experiments were performed under atmospheric pressure in a thermostated water bath equipped with a shaker (Electra medical corporation , SWB 402). The water bath was adjusted at 25°C. In all the experiments, the solid and liquid samples were placed in sealed polypropylene tubes.

The UV-Visible absorbance readings of the liquid and supernatant phases were recorded using a Varian carry 50 spectrophotometer at λ_{max} of 350 nm. The concentrations of chromium were determined from the calibration curve prepared previously (Appendix A).

2.6.1 Effect of time

In the kinetic experiments, 0.10 g samples of Fe NPs (nZVI) were mixed with 25.0 ml aliquots of 100 mg/L Cr (VI) solution, and were contacted for 1 min, 5 min, 30 min, 1 hr ,4 hr and 24 hr.

The Cr (VI) solutions were separated from Fe NPs by centrifugation (Labo fuge 200) and / or filtration. The supernatant solutions were analyzed by measuring the UV-Visible absorbance of the solutions.

In addition to the previous experiment, a blank experiment was also carried out in parallel at the same Cr (VI) concentration (100 mg/L), using zeolite and Z-nZVI composites. The contact times were kept as above, and the Cr (VI) solutions were separated and analyzed in the same way as in the nZVI experiment.

2.6.2 The effect of initial Cr (VI) concentration

In the related experiments, the initial Cr (VI) concentrations were 5.0, 10.0, 25.0, 50.0, 100.0 mg/L. In each trial, 0.1 g samples of nZVI were added to 25.0 ml Cr (VI) solution portions and were mixed for 1 hr in a shaker kept at 25°C.

The Cr (VI) solutions were then separated from nZVI using centrifugation and/or filtration, and were analyzed by measuring the UV-Visible absorbance. The pH of the solutions was measured using a pH-meter (HANNA instrument, HI 98129, HI 98130).

The effect of concentration was studied also for pure zeolite and Z-nZVI composites. The same initial Cr (VI) concentrations and time of contact were used and the solutions were separated and analyzed in the same way reported in the previous section.

2.6.3 Effect of initial pH on the Cr (VI) removal

The effect of the pH on the removal of Cr (VI) by nZVI was studied at 100 mg/L initial concentration. In each trial 0.1 g of nZVI was added to 25.0 ml of the Cr (VI) solution and the pH was adjusted to 2.0, 4.0, 6.0, 8.0 and 10.0. The samples were left in contact with the solutions for 2 hr, the solutions were then separated via filtration, and the supernatants were analyzed by measuring the UV-Visible absorbance and pH of the samples.

The experiment reported above was repeated in the same way by replacing nZVI with Z-nZVI.

2.7 Plant experiments - Effect of Fe NPs on Corn growth

2.7.1 The experiment layout

The corresponding experiments were performed using 25-L pots made from polyethylene plastic which is usually used in farming.

The experimental design used was a randomized completely blocks design (RCBD), with twelve treatments each replicated five times (there were 60 experimental units as shown in Figure 3 and Figure 4).

Experimental Layout (5 block)

A	10	2	1	4	5	6	8	9	11	12	3	7
B	11	3	6	2	12	1	10	8	9	7	4	5
C	11	2	3	9	12	7	10	8	4	1	5	6
D	8	9	12	6	10	11	3	7	2	1	5	4
E	5	4	1	3	10	8	7	11	2	6	9	12

Figure 3 The plant experiment layout (RCBD)



Figure 4 An image of the planting site

Table 4 shows the twelve treatments included.

Table 4 Treatments included in the plant experiment

Treatment	Classification
1	Positive control (soil + Cr (VI))
2	Negative control (only soil)
3	Zeolite 0.1 mg / Kg + Cr (VI) 200 mg / Kg
4	Zeolite-nZVI 0.2 mg / Kg + Cr (VI) 200 mg / Kg
5	nZVI 0.1 mg / Kg + Cr (VI) 200 mg / Kg
6	GT-Fe 0.1 mg / Kg + Cr (VI) 200 mg / Kg
7	GT-Fe 1 mg / Kg + Cr (VI) 200 mg / Kg
8	Zeolite 0.1 mg / Kg
9	Zeolite-nZVI 0.2 mg / Kg
10	nZVI 0.1 mg / Kg
11	GT-Fe 0.1 mg / Kg
12	GT-Fe 1 mg / Kg

2.7.2 Preparing soil for planting

Pots were filled with a soil-sand-pitmos mixture (soil mix) at a ratio of 4:1:0.5, respectively. The capacity of the planting pot was determined and calculated as 24.5 Kg. For each treatment, the amount of soil mix and the exact weights of chemicals needed in each treatment were calculated and weighed, then mixed manually after adding enough amount of tap water to result in as possible as a homogenous mixture in a large vessel. Then the mixtures were distributed in the five pots related to the five replicates of the treatments. The pots were then left for one week to allow the soil mix and chemicals to equilibrate with each other as much as possible.

2.7.3 Planting

Corn was chosen as a model plant in the corresponding experiments. Corn seeds were planted on 9/7/2014, with two seeds planted in each pot. The first set of soil samples was collected in the same day at the beginning of the planting. The pots were irrigated regularly with tap water 2-3 times per week. In each time, for each pot, 2-3 L of water was added.

After about two months (on 18/9/2014), at the middle of the planting period, the second set of soil samples were collected, and observations on the plant growth and progress were recorded for future comparisons.

2.7.4 ICP-OES analysis for soil samples

Inductively Coupled Plasma-Optical Emission Spectrometry (ICP-OES) analysis was performed at the Center of Birzeit University Testing Labs.

Soil samples were collected at the beginning and at the middle period of planting (after two months). All samples were collected from the top soil sections and were analyzed with ICP-OES to determine and compare the concentrations of iron and chromium in the twelve treatments.

The metal analysis for the soil samples was performed as follows; the soil samples were dried to remove moisture (each soil sample was kept in a tray at 70°C over night), and the samples were then sieved at 60 mesh sieve (0.250 mm) to allow 200 mg from the soil to pass through the sieve into a crucible.

Each sample was digested with around 20 ml of Aqua-regia (HCl+HNO₃ at 3:1 v/v ratio), and boiled on a hot plate. Volume reduction in each sample occurred (sample size with aqua regia became below 5 ml due to evaporation and digestion).

After digestion was completed, the crucible was cooled and the remaining was filtered with a 0.45 micrometer filter, and transferred to 50 ml volumetric flask. Distilled water was added to the filtrates up to total volume of 50 ml (total volume of sample and distilled water), and the samples were then analyzed by ICP-OES.

2.8 Effect of Fe NPs on Bacteria

The antibacterial activity of Fe NPs (nZVI) was investigated on bacteria types present in soil.

The samples, solution concentrations and bacteria types used in these experiments are given in Tables 5 and 6, and pictures of the well plates are shown in Fig. 5.

Table 5 Samples which were tested in the bacteria experiments

Sample	Concentration (mg/L)
Chromium solution (Cr(VI))	10
Chromium solution (Cr(VI))	100
nZVI slurry	10
nZVI slurry	50
GT-Fe slurry	10
GT-Fe slurry	50
(Cr(VI)) solution + nZVI	100 Cr/50 iron
(Cr(VI)) solution + GT-Fe	100 Cr/50 iron

Table 6 Types of tested Bacteria

#	Bacteria name
1	<i>Escherichia coli</i>
2	<i>Klebsiella pneumonia</i>
4	<i>Staphylococcus aureus</i>
5	<i>Bacillus subtilis</i>

The chemicals were added to bacteria as shown in Table 7.

Table 7 Presentation of the type and order in which chemicals were added to the 24 well plates (each well contains the tested bacteria)

	1	2	3	4	5	6
A	Empty (Only bacteria)	Empty (Only bacteria)	Cr(VI) solution 10 mg/L	Cr(VI) solution 10 mg/L	Cr(VI) solution 100 mg/L	Cr(VI) solution 100 mg/L
B	nZVI slurry 10 mg/L	nZVI slurry 10 mg/L	GT-Fe slurry 10 mg/L	GT-Fe slurry 10 mg/L	(Cr(VI)) solution (100) + nZVI (50)	(Cr(VI)) solution (100) + nZVI (50)
C	nZVI slurry 50 mg/L	nZVI slurry 50 mg/L	GT-Fe slurry 50 mg/L	GT-Fe slurry 50 mg/L	(Cr(VI)) solution (100) + GT-Fe (50)	(Cr(VI)) solution (100) + GT-Fe (50)

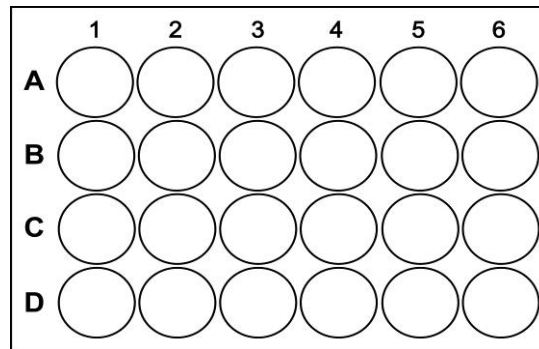
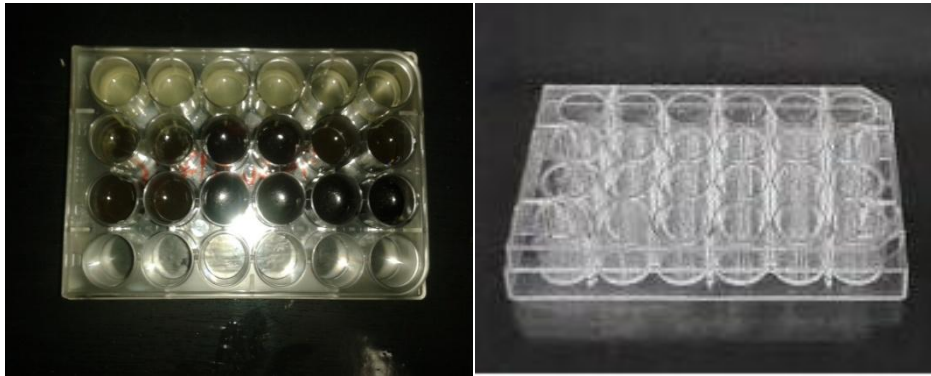


Figure 5 Different pictures of the 24 well plates used in the bacteria experiments

2.8.1 Procedure

The medium was prepared by dissolving 38.0 g of Mueller Hinton Agar No.2 in 1L of distilled water. The solution was heated to boiling to dissolve the medium completely and sterilized by autoclaving at 120°C, 15 lbs pressure for 2 hrs. Then it was mixed well and poured into sterile Petri dishes using aseptic conditions. Base layer was obtained by pouring around 20–30 ml of Muller Hinton Agar solution

to obtain a thickness of 4 mm. It was then kept for solidification.

Subsequently, the following steps were performed:

- 1- Bacterial suspension was prepared and standardized to a 0.5 Mcfarland density in 0.9 % saline (1.5×10^8 CFU/ml).
- 2- 0.5 ml of Muller Hinton Broth were taken in each well in the 24 well plate (Fig. 2-3), 100 μ l of the standardized prepared bacteria were added to each well, then the specific chemicals were added to the plate as described in Table 2-6.
- 3- The four 24 plate well, each containing one type of the mentioned bacteria types were incubated at 37°C with shaking overnight.
- 4- In the next day, serial dilution of bacteria were done before spreading 50 μ l of each well on muller Hinton Agar for counting.

Finally, counting was performed.

3. Results & Discussion

3.1 Characterization of Fe nanomaterials

This section is devoted to providing the results of the characterization experiments performed for Fe nanomaterials and soil samples used in this work. The results include SEM/EDX, TEM, XRD, and XRF results.

3.1.1 Characterization of nZVI

Nano-zero-valent iron produced using borohydride reduction method was characterized to reveal its morphology, phase type(s), and elemental content. The SEM image provided in Fig. 6 indicate that the material posses its chain-like structure, in accordance with previous results [22]. nZVI is well known to demonstrate this morphology due to the strong magnetic attractive forces between the nanoparticles, each of which has a core-shell structure, with the core consisting of Fe^0 , while the shell is composed of iron oxides and oxyhydroxides [77].

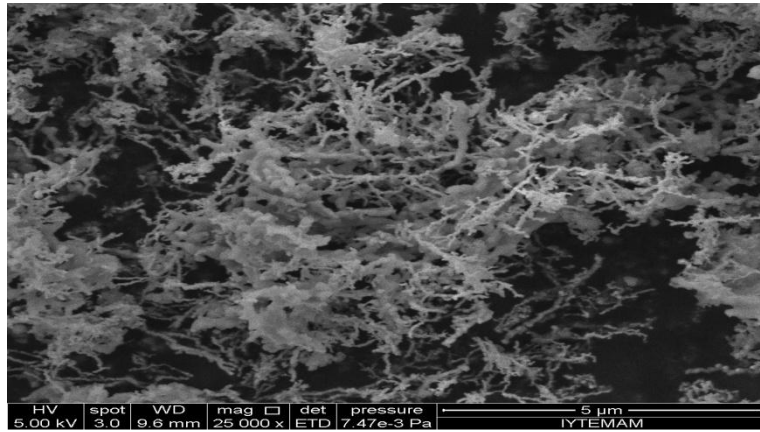


Figure 6 SEM image of nZVI aggregates showing its chain like structure.

The material was characterized also using TEM, as shown in Fig. 7. The images of nZVI reveal the formation of aggregates and chain like structure of iron nanoparticles. According to this analysis, the diameter of the individual nanoparticles ranges between 20 and 70 nm.

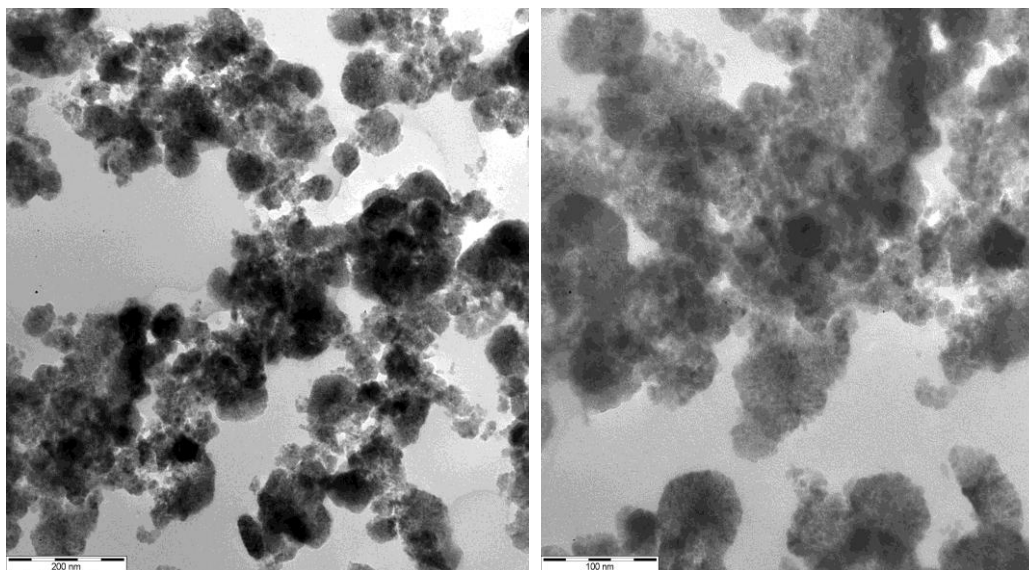


Figure 7 TEM images of nZVI at two different scales (a-200 nm, b-100 nm)

The formation of nZVI was also documented using XRD analysis, which shows its characteristic peak at 44.9° . The peak shown in Fig. 8 looks somewhat broad and its intensity is weak suggesting limited crystallinity in the material. It is important to notice that no peak of iron oxide exists, indicating that no oxidation of the material took place during synthesis and subsequent storage, prior to using them in the removal of Cr(VI) ions.

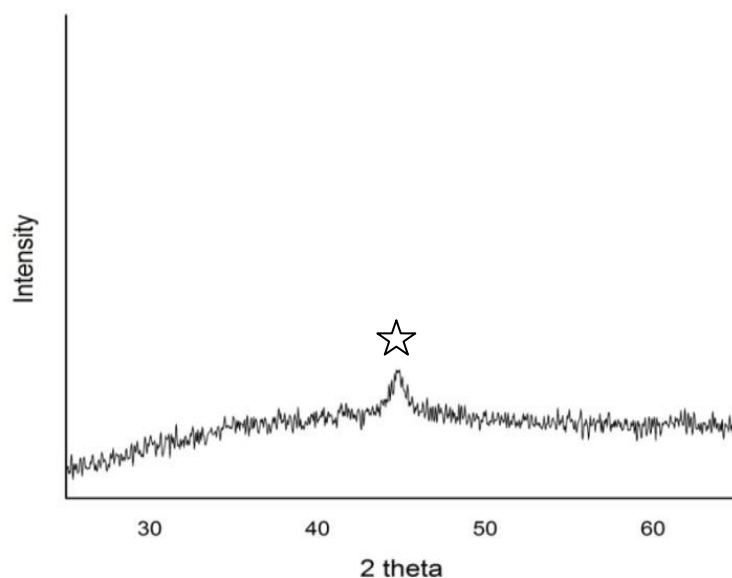


Figure 8 XRD pattern of nZVI

The elemental content of nZVI was tested using XRF, as given in Table 8 on oxygen-free basis. The characterization results are shown in integrated mode in Table 8 where the % composition by weight for characterized elements are given. The data shows that the nZVI is dominated by Fe element, with a considerable amount of Na originating most probably from the NaBH_4 used as a reducing agent during the synthesis of nZVI.

Table 8 XRF analysis results for nZVI

Element	% Composition by weight
Sodium (Na)	8.9
Chromium (Cr)	0.0
Iron (Fe)	86.9
Others *	4.2
Sum	100.0

*Others are elements found in the sample in very small amount (less than 1 %).

3.1.2 Characterization of zeolite-nZVI composite

The synthesis procedure of this material (named shortly as Z-nZVI) was reported earlier by Muath Nairat and coworkers, and detailed characterization has been performed [67]. This material was employed in this work to compare its behavior with that of nZVI when used alone.

Zeolite used in this study as a solid support for nZVI was obtained from a natural source located in Turkey. The chemical structure consists mainly of sodium, potassium, calcium, and aluminasilicate.

The mineralogical structure is composed mainly of Clinoptilolite, which is the most widely available natural zeolite [68].

As shown in Fig. 9, nZVI retains its characteristic chain-like structure when synthesized in the presence of zeolite material, however, the main advantage of using zeolite is to decrease the nZVI aggregation in aqueous media, as nZVI is well known to aggregate tremendously and settles down in water very rapidly when used alone.

The formation of nZVI in its Fe^0 state is also verified using XRD, as shown in Fig. 10. The major feature arising at 44.9° is indicative of that.

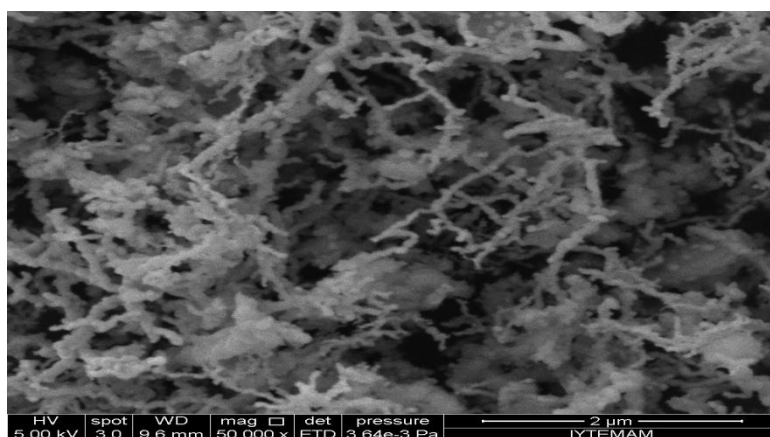


Figure 9 SEM image of Z-nZVI (1:1 ratio of zeolite and Fe^{2+} ions)

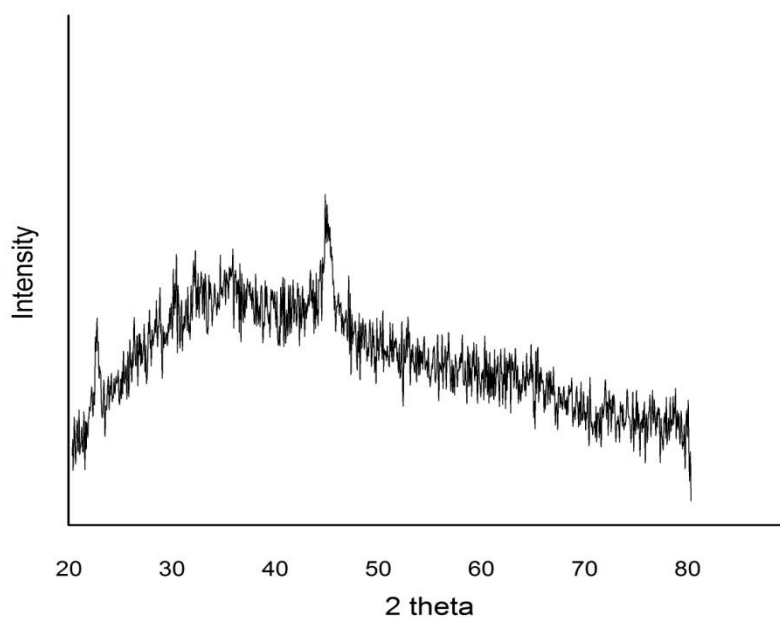


Figure 10 XRD pattern of Z-nZVI

3.1.3 Characterization of “greener” nano iron

In addition to the nZVI produced via borohydride reduction, nano iron has been produced by exposing Fe^{2+} ions to extracts of green tea. This procedure aims at synthesizing greener iron nanoparticles, in which the tea extract acts as a reducing and a capping agent, thus eliminating the need for using chemicals (for example reducing agent like sodium borohydride) for these purposes [69].

The samples produced by this method are named GT-Fe NPs, and were employed in this study to compare the extent of removal of

Cr(VI) from soil once when nZVI is applied, and once when GT-Fe NPs is applied, in search of a better remediation.

The formation of GT-Fe NPs could not be verified using SEM analysis due to their small size, however, TEM images indicated the formation of nanoparticles the size of which is around 5-10 nm as shown in Fig. 11.

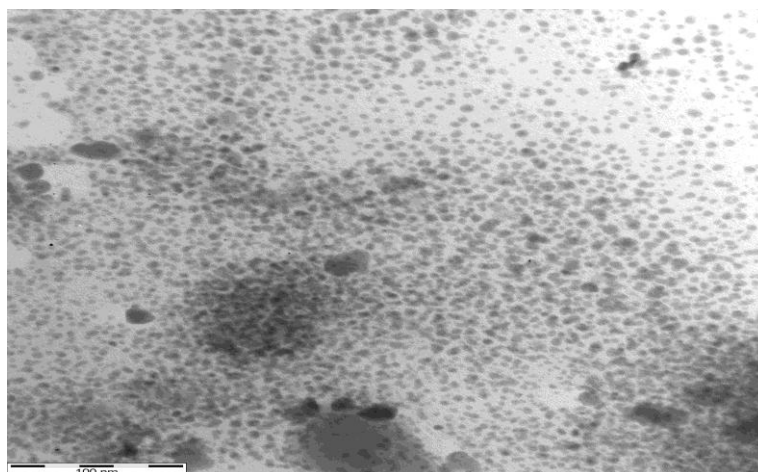


Figure 11 TEM image of GT-Fe NPs.

The GT-Fe NPs was also characterized by XRD as shown in Fig. 12. The formation of zero-valent-iron phase is indicated by the reflection appearing at 45° . This reflection seemingly overlaps with the (220) reflection of NaCl, which appears to extensively during the synthesis process. The salt formation is verified by the sharp reflections

appearing at 2θ values of 27.2, 31.5, 45.3, 56.3, 66.1, 75.1 standing for the hkl planes of 111, 200, 220, 222, 400, 420, respectively [78].

The XRF analysis of the elemental content indicates, in addition to Fe, a rich content of Na (originating from NaOH used during the synthesis) and Cl (originating from the chloride salt of iron) elements, and small amounts of K, Mg, Al originating mainly from the green tea extract.

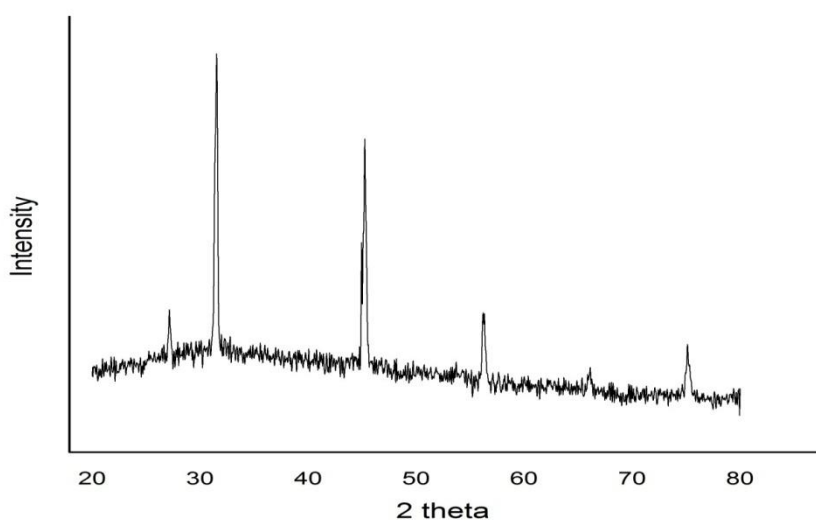


Figure 12 XRD pattern of GT-Fe NPs.

Table 9 XRF analysis results for GT-Fe NPs.

Element	% Composition by weight
Sodium (Na)	52.4
Magnesium (Mg)	4.2
Aluminium (Al)	2.1
Chlorine (Cl)	17.4
Potassium (K)	5.0
Chromium (Cr)	0.0
Iron (Fe)	17.9
Others	1.0
Sum	100.0

3.1.4. Characterization of the soil samples

A typical SEM image of the soil grains is shown in Fig. 13, and an XRD diagram is given in Fig. 14. The XRD analysis reveals multiple reflections which points to the complex mineralogical content of the soil, but it is readily distinguished that the main component is quartz

(SiO₂), as evident from the major reflections occurring at 2θ values of 20.8, 26.6, 36.5, 50.1, and 59.9 [79].

The elemental content analysis performed using EDX and shown in Fig. 15 indicates the presence of the major elements O, C, Si, Al, Fe, Ca, Mg, K, with atomic percentages of 59.1, 23.7, 7.7, 3.8, 1.4, 1.9, 1.5, 0.5, respectively.

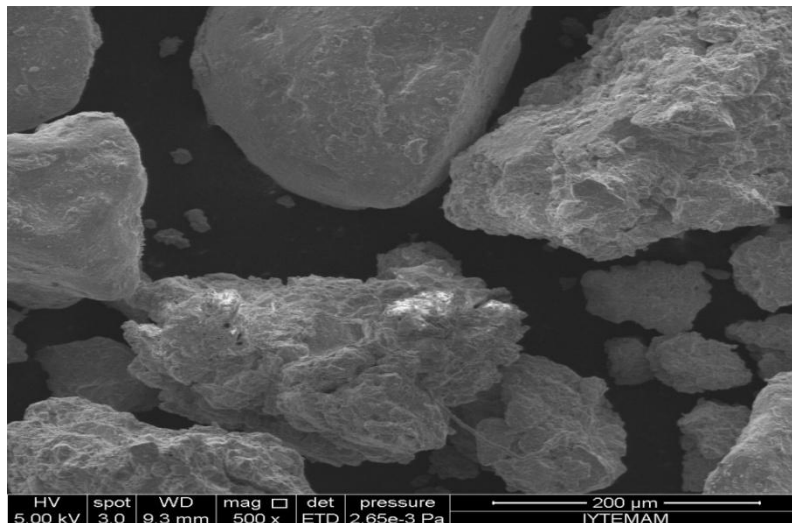


Figure 13 A typical SEM image of soil grains.

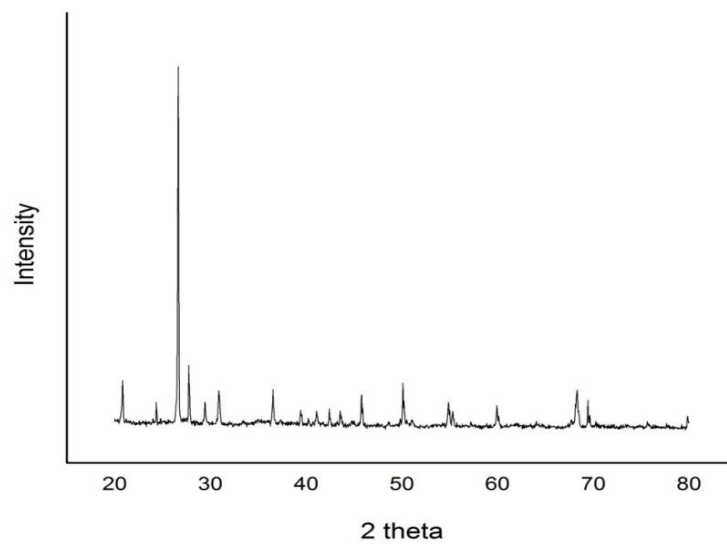


Figure 14 XRD pattern of a soil sample.

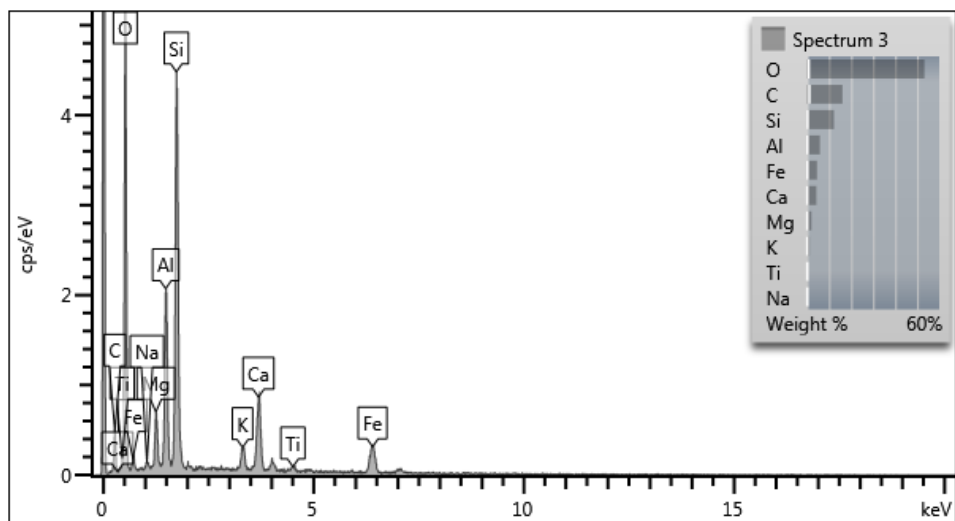


Figure 15 Elemental content of a typical soil sample.

In addition, the BET and Langmuir surface areas of soil were determined. The obtained values were 29.8 and 38.6 m²/g. When the soil samples were mixed with GT-Fe NPs, the surface area increased to 37.8 (BET) and 48.8 m²/g (Langmuir). Moreover, SEM images showed that mixing the soil samples with GT-Fe NPs resulted in increasing the surface roughness of soil, and so the soil surface increased. A typical image is given in Fig. 16.

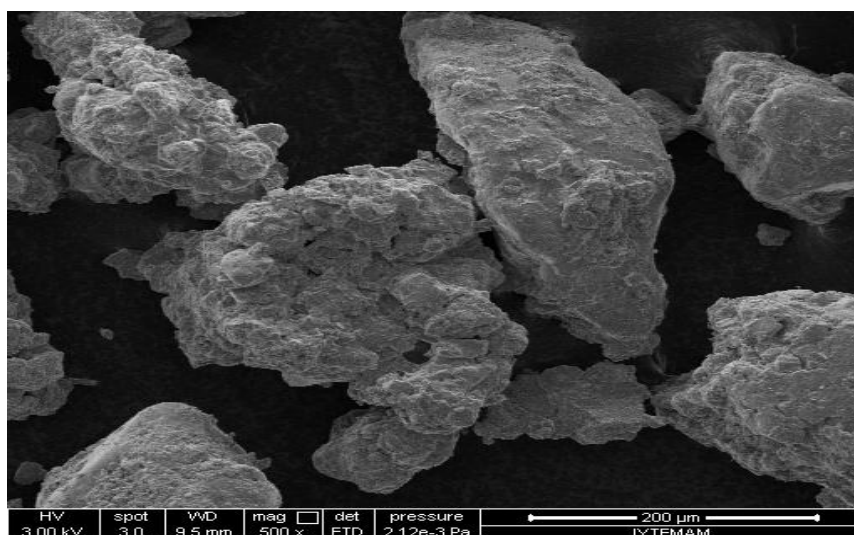


Figure 16 A SEM image of a mixture of Soil and GT-Fe NPs.

In the following sections, the removal of Cr(VI) using iron nanomaterials will be presented and discussed. First, the removal studies of Cr(VI) in aqueous solutions will be considered. Then, the removal of Cr(VI) from soil mixed with Fe NPs will be addressed, and

the effect of these NPs on corn growth will be discussed. Corn was selected as a model plant. Finally the effect of Fe NPs on bacteria types (commonly found in soil) will be addressed.

3.2 Removal of Cr (VI) from aqueous solution

In this part of the study, the extent of removal of aqueous Cr(VI) ions by nZVI has been investigated as a function of time, concentration and pH. For the sake of comparison with nZVI, the experiments were also repeated using Z-nZVI as an adsorbent.

The concentration of Cr(VI) in aqueous solutions was determined using UV-Visible spectrophotometry. The details are given in the following sections.

3.2.1 Calibration curve

The calibration curve constructed and used in this study is provided in appendix A. The linear relationship of this curve is given as: $y = 0.030x - 0.002$, where x stands for the concentration of Cr(VI) in mg/L, and y stands for the UV-Vis. Absorbance. The coefficient of determination (R^2) for the linear relationship was 0.9990, indicating very high linear correlation in the applied concentration range.

3.2.2 Effect of time

The effect of time on the extent of removal of aqueous Cr(VI) ions was studied at initial ion concentration of 100 mg/L for a period ranging from several minutes up to 24 hours. The change in concentration with time is given in Fig. 17, and the change in the amount of adsorbed Cr(VI) on nZVI with time is given in Fig. 18. This amount was calculated using the well known mass balance equation [80],[81] :

$$Q = (C_o - C) \frac{V}{m} \dots\dots\dots (1)$$

Here Q is the adsorbed concentration of Cr(VI) in mg/g, C_o and C are the initial and final concentrations of aqueous Cr(VI) ions in mg/L, V is the solution volume (L), and m is the mass of nZVI (g).

As seen from the data, equilibrium is approached rapidly, in about one hour of contact between liquid and solid phases.

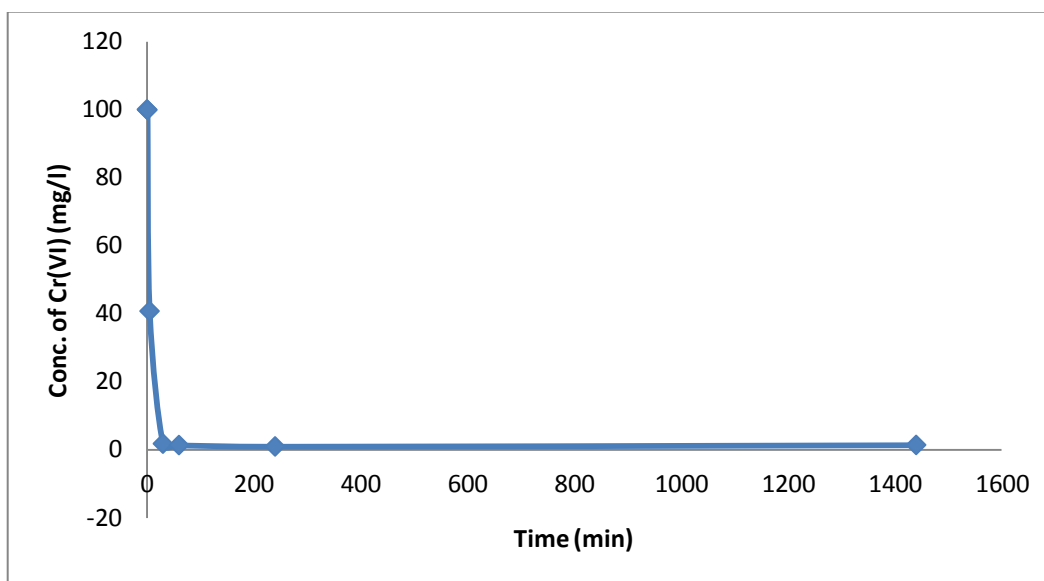


Figure 17 Variation of Cr(VI) aqueous concentration with time upon contact with nZVI.

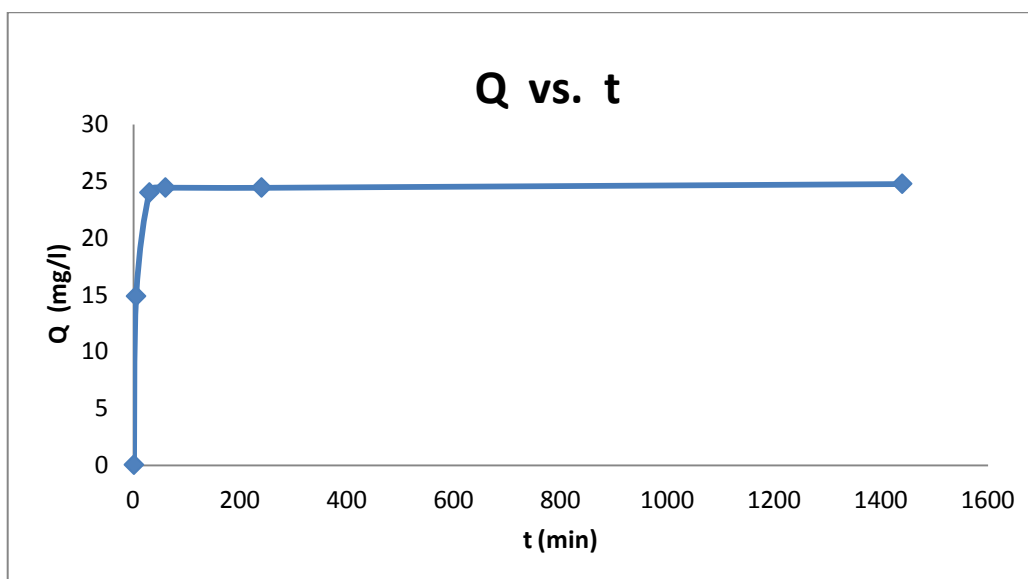


Figure 18 Variation in the adsorbed amount of Cr(VI) on nZVI with time.

The same experiment was repeated using Z-nZVI instead of nZVI. The variation of aqueous Cr(VI) concentration with time is shown in Fig. 19. The obtained results indicate that the removal process is slower in this case compared with nZVI, as more than four hours seems to be required to attain equilibrium (after these four hours of contact, no significant change in the Cr(VI) concentration occurred). This is most probably caused by the large internal area of the zeolite material which leads to a diffusion barrier.

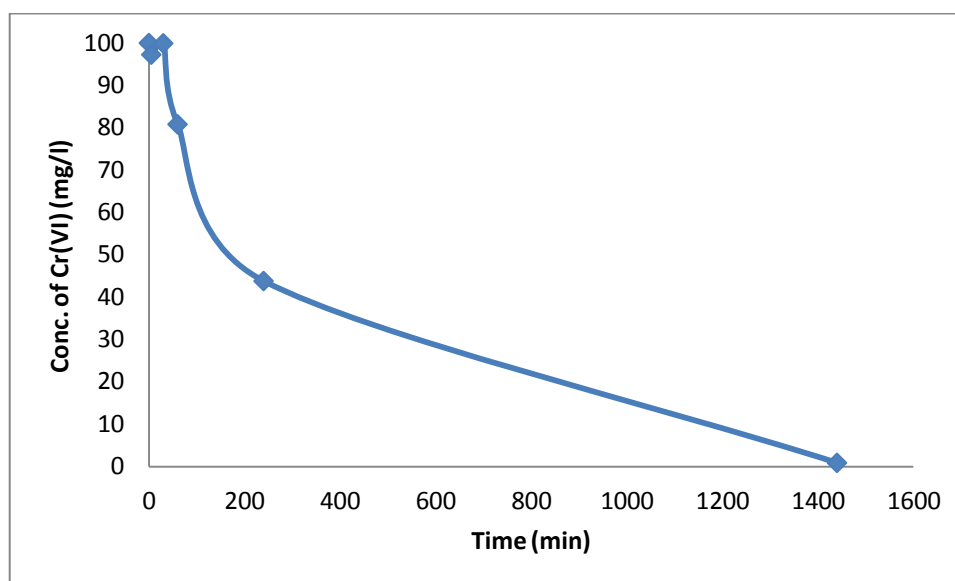


Figure 19 Variation of Cr(VI) aqueous concentration with time upon contact with Z-nZVI.

The sorption data were fitted to pseudo first order kinetics expressed in the following equations [81] :

$$\ln(Q_{max} - Q) = \ln Q_{max} - k_1 t \dots \dots \dots (2)$$

Here, k_1 stands for the rate constant, t is the time, and Q_{max} is the maximum sorbable amount, given by the relation:

$$Q_{max} = C_o \frac{V}{m} \dots \dots \dots (3)$$

The data is plotted in Fig. 20. The coefficient of determination (R^2) was 0.9980, indicating a very well linear correlation. The value of k_1 was calculated as $3.4 * 10^{-3} \pm 0.2 * 10^{-3} \text{ min}^{-1}$, and Q_{max} (maximum sorbable amount) found as $24 \pm 1 \text{ mg/g}$.

For a first order reaction, the half life time $t_{1/2}$ is $\ln 2/k_1$, and using this relation $t_{1/2}$ of the removal reaction was found to be 231 min. This was confirmed experimentally by performing a time effect experiment with the same parameters and time of contact equal to $t_{1/2}$, the equilibrium concentration measured after this time decreased from 100.0 mg/L to 45.9 mg/L, almost half the initial concentration.

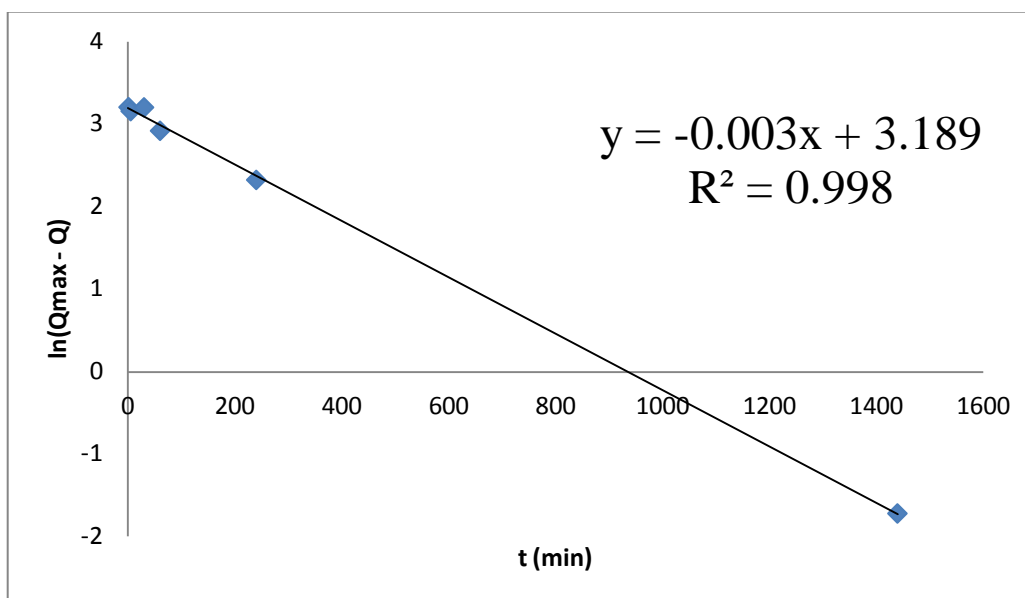


Figure 20 Pseudo-first order plot of the removal of Cr(VI) by Z-nZVI

It must be mentioned that another experimental set was performed using pure zeolite in order to check the contribution of zeolite to the removal process. The results showed negligible removal of Cr(VI) by zeolite under the studied conditions. This observation leads to the conclusion that Cr(VI) removal by Z-nZVI composite is achieved by virtue of iron nanoparticles.

3.2.3 The effect of initial Cr (VI) concentration

In this section, the effect of loading of Cr(VI) ions was studied at the initial concentrations of 5.0, 10.0, 25.0, 50.0, and 100.0 mg/L.

Throughout these experiments the time of contact was kept as 1 hr.

The experiments were performed using nZVI as a sorbent, and were then repeated using Z-nZVI under the same conditions.

The results of the experiments are provided in Figs. 21 and 22.

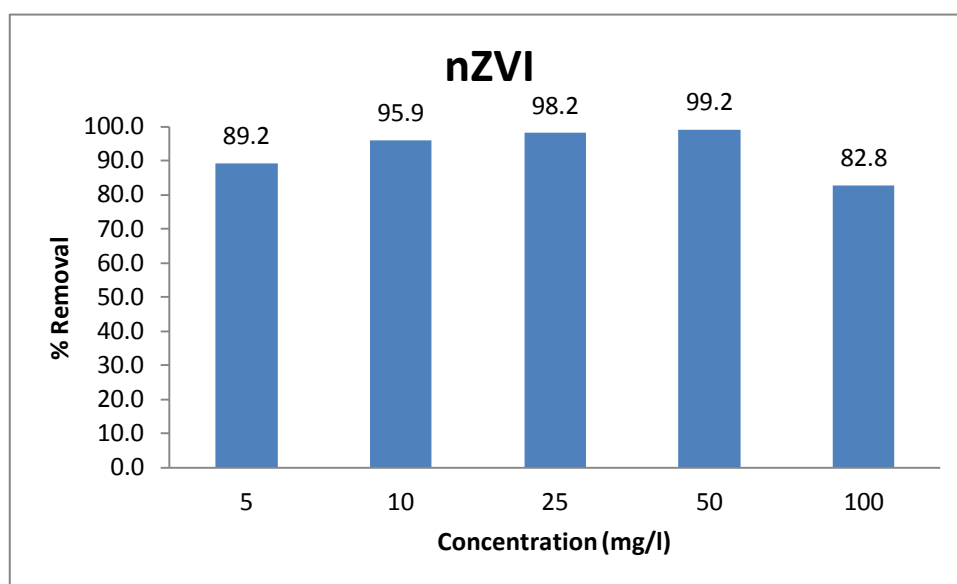


Figure 21 The effect of initial Cr(VI) concentration on the removal of Cr(VI) by nZVI.

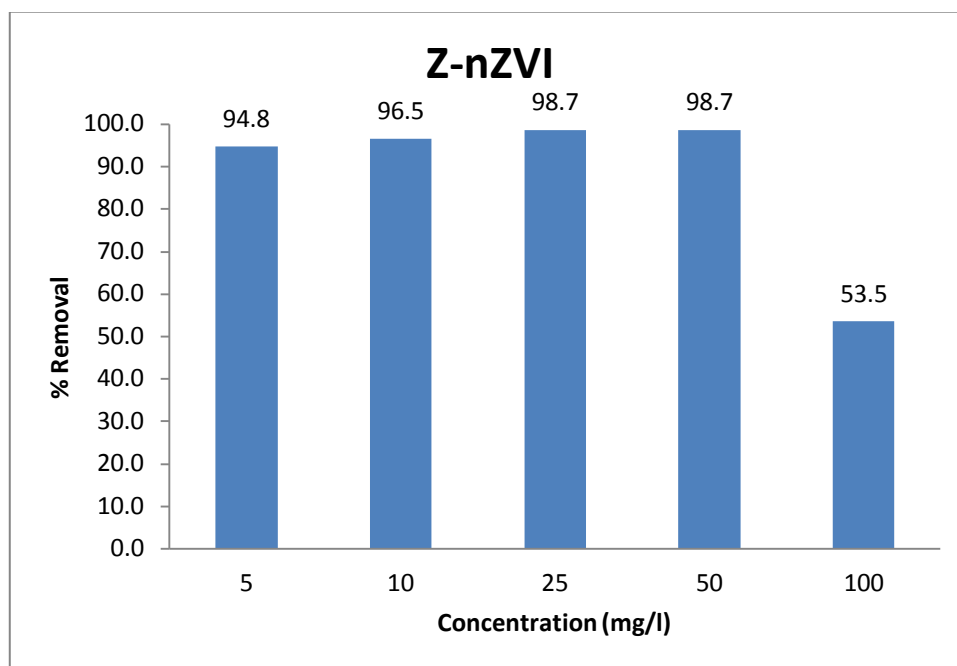


Figure 22 The effect of initial Cr(VI) concentration on the removal of Cr(VI) by Z-nZVI.

The percentage removal was calculated using the equation:

$$\% \text{ Removal} = \frac{c_o - c}{c_o} \times 100 \dots\dots\dots (4)$$

In both cases, the extent of removal is smallest at 100 mg/L, although the value corresponding to Z-nZVI is much smaller than that of nZVI.

Below this concentration, the percentage removal appears to reach about 90% or more. This reflects the high removal potential of both of nZVI and Z-nZVI materials against Cr (VI).

Tables 10 and 11 show the pH values for Cr(VI) solutions measured at the beginning and at the end of the reaction with nZVI and Z-nZVI respectively, with changing the initial Cr(VI) concentration each time.

Table 10 pH values measured at the beginning and the end of the reaction of Cr(VI) with nZVI

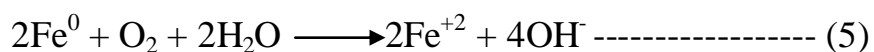
Cr(VI) conc. (mg/L)	pH initial	pH final
100	5.31	9.15
50	5.53	9.09
25	5.77	8.90
10	6.06	8.87
5	6.13	8.82

Table 11 pH values measured at the beginning and the end of the reaction of Cr(VI) with Z-nZVI

Cr(VI) conc. (mg/L)	pH initial	pH final
100	5.31	8.75
50	5.53	8.81
25	5.77	8.71
10	6.06	8.52
5	6.13	8.45

The pH values for both nZVI and Z-nZVI increased at the end of the reaction, this is an indication that iron was oxidized through the reactions.[49]

The oxidation of Fe^0 in aqueous systems releases OH^- ions, increasing the pH of the system (>8.0) as shown in Eq. (5) [6].



3.2.4 Effect of pH of the Cr (VI) solution

The effect of solution pH on the extent of removal of Cr(VI) by nZVI and Z-nZVI was studied over a wide range of pH; from 2.0 to 10.0.

The time of contact throughout these experiments was 2 hrs. The obtained results are given in Figs. 23 and 24.

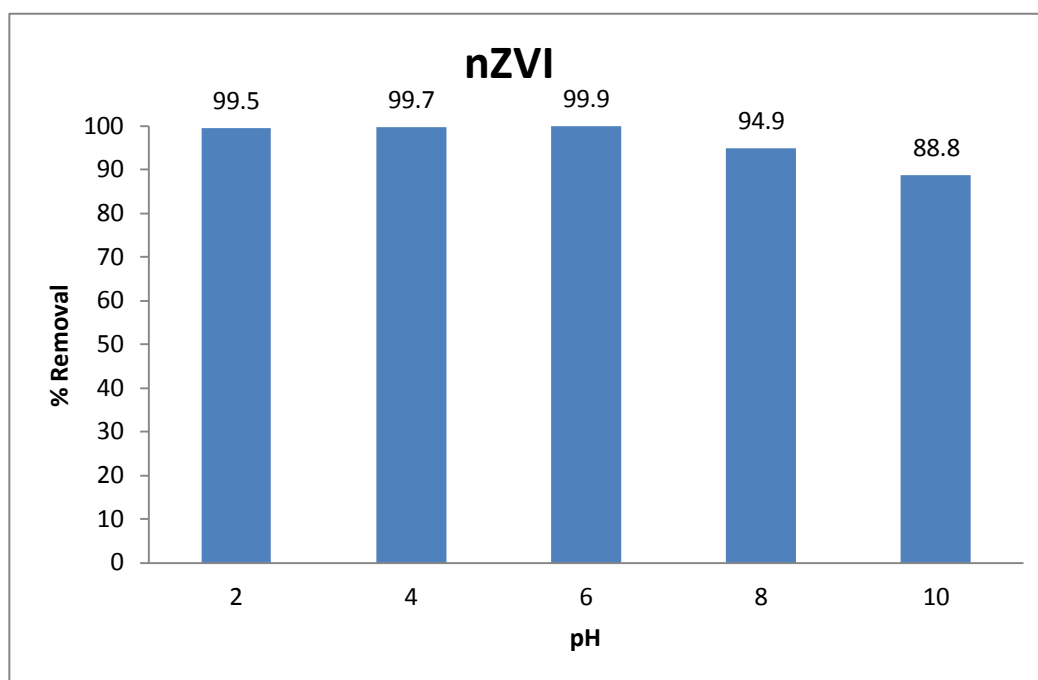


Figure 23 Effect of initial solution pH on the extent of Cr(VI) (100 mg/l) removal by nZVI.

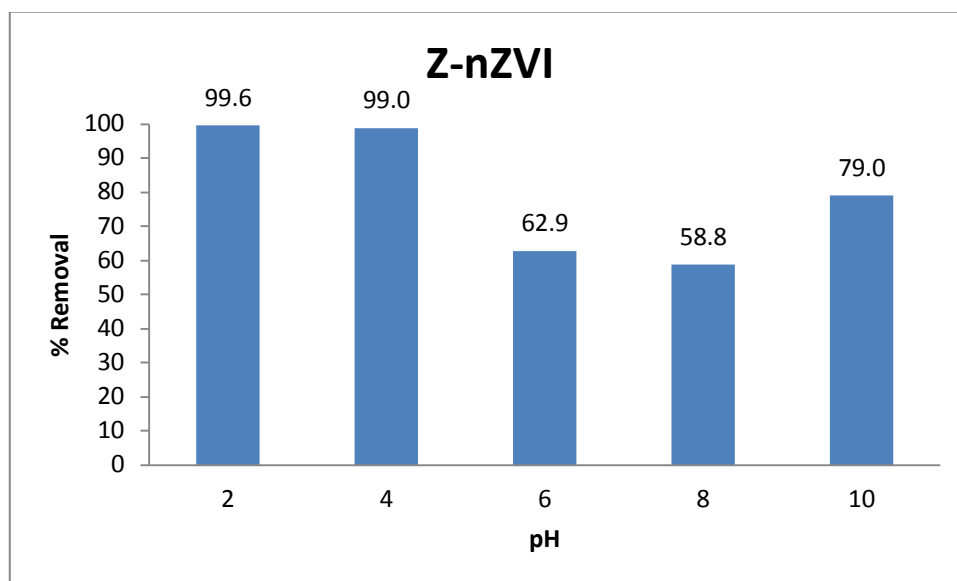


Figure 24 Effect of initial solution pH on Cr(VI) (100 mg/l) removal by Z-nZVI.

As seen in Fig. 23, the removal percentage of Cr(VI) decreased from 99.5% to 88.8% when the initial pH of solution was increased from 2.0 to 10.0. This suggests that the removal of Cr(VI) is slightly dependent on the initial pH of the solution [83].

The effect of pH on the % of removal of Cr(VI) is obvious when pH is increased beyond 6.0. The % removal was around 99.5% for pH 2, 4 and 6, indicating almost complete removal under the studied conditions. But for pH=8.0, the % removal decreased to about 95%, and continued to decrease to 89% at pH=10.0.

In the case of Z-nZVI, the removal process is seen to be more sensitive to the pH, especially in the alkaline range.

The removal of Cr(VI) is high over a wide range of pH values, this is significant as soil pH is considered a master variable in soils since it controls many chemical processes. It specifically affects plant nutrient availability by controlling the chemical forms of the nutrient. The optimum pH range for most plants is between 5.5 and 7.0 [82].

In general, the higher removal in the acidic medium could be related to solubilisation of iron [84]. At lower pH values, the high concentration of H^+ causes corrosion of nZVI particles [83], leading to formation of oxide and oxyhydroxide products which can be effective in the surface fixation of chromate specie by chelation reactions.

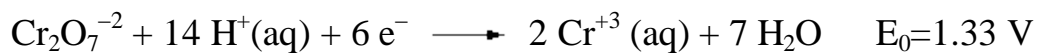
A further explanation for this behaviour could be provided based on the speciation of Cr(VI) specie and the zero point of charge (ZPC) of iron oxide and oxyhydroxide which lie in the basic pH range. By inspecting the speciation products of Cr(VI) ion in aqueous media it is clear that all of them carry a negative charge. The dominant Cr(VI) species in acidic medium is $HCrO_4^-$, while the dominant specie is CrO_4^{2-} and $Cr_2O_7^{2-}$ [85]. On the other hand, in the acidic medium, the surface of Fe nanoparticles (containing -OH, -OOH groups) will be

protonated, i.e. carry a positive charge, and this makes it possible for chromate specie to be attracted by the surface and eventually adsorbed.

The removal mechanism of Cr(VI) ions by nZVI is a complex one. In addition to the pH-dependent removal of Cr(VI) by surface groups of nZVI, pH-independent removal of Cr(VI) can take place. It has been reported that Cr(VI) can form monodentate and bidentate (mononuclear and binuclear) inner sphere complexes with iron hydrous oxide surface [86]. A schematic representation of this is shown in Fig. 25.

Another reported mechanism for Cr(VI) removal by nZVI is its reduction to Cr(III) by the electron supported from the core of iron nanoparticles [87]. nZVI is well-known for its core-shell structure, with the core composed of Fe^0 , and the shell composed of iron oxide and oxyhydroxide groups, as mentioned above. The core forms a source of electrons ($\text{Fe}^0 \longrightarrow \text{Fe}^{+2} + 2\text{e}^-$), and these electrons can reduce a wide range of inorganic ions as reported in literature. The precondition for this is that the particular ion possesses an electrode potential that is higher than that of Fe. In the case of Cr(VI), this

condition is fulfilled as seen in the following reactions, and their corresponding standard reduction potential [88]:



The redox reaction can then lead to sorption of the produced Cr(III), or precipitation of its hydroxide, depending on the operating conditions and the type of sorbent.

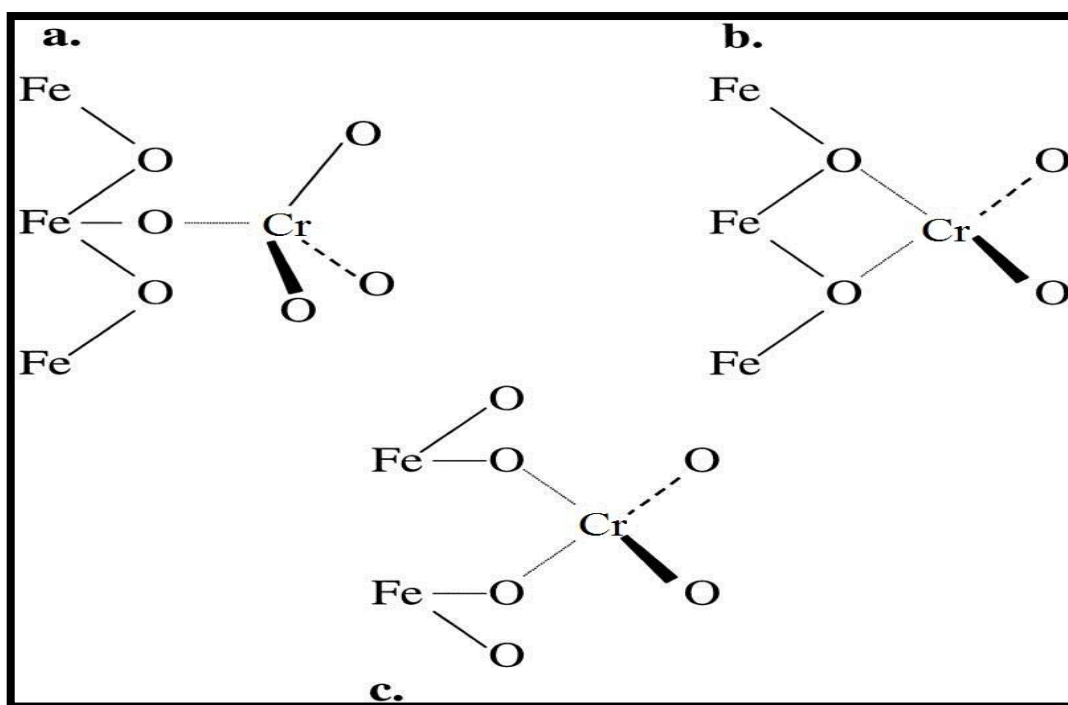


Figure 25 A schematic representation of (a) monodentate and bidentate ((b) mononuclear and (c) binuclear) inner sphere complexes that Cr(VI) can form with iron hydroxide surface [86].

3.3 Effect of Cr(VI) removal from soil mixed with Fe NPs on Corn growth

In this part of the study, the removal of Cr(VI) from soil was studied, and the effect of the removal process on plant growth was investigated. Corn was selected as a model plant for this purpose.

3.3.1 Removal of Cr(VI) from soil mixed with Fe NPs

Prior to examining the effect of Cr(VI) contamination and iron nanoparticles on the growth of corn, the soil samples mixed with GT-Fe NPs were characterized by surface techniques to check the fixation of Cr(VI) by Fe NPs.

As was mentioned previously, BET and Langmuir surface areas of soil increased upon mixing it with GT-Fe NPs from 29.8 m²/g to 37.8 m²/g for BET, and from 38.6 m²/g 48.8 m²/g for Langmuir, increased surface area result in higher removal efficiency against Cr(VI). Moreover, SEM images showed that mixing the soil samples with GT-Fe NPs resulted in increasing the surface roughness of soil, as was shown in Fig. 16.

Mixture of soil and Fe NPs were analyzed before and after Cr(VI) removal using EDX, XRD, and TEM.

The EDX analysis was performed using the electron mapping mode in order to reveal the distribution of Cr(VI) on the sample mixture of soil and Fe NPs. Here, the positions of specific elements emitting characteristic x-rays within an inspection field can be indicated by unique color. The results are shown in Fig. 26 where the maps of Si, Fe, and Cr are shown individually. The Si element represents the soil part as it was found to be the major element in soil. The results showed that the Cr signals are better associated with the Fe signals than with Si.

Cr(VI) is known to be very mobile in soil. The specie of Cr(VI) include CrO_4^{2-} , HCrO_4^- , and $\text{Cr}_2\text{O}_7^{2-}$, and due to the anionic nature of these specie, Cr(VI) cannot be retained by the anionic groups of soil (SiO_2). Its sorption on soil is largely related with the Fe and Al hydrous oxide content of the soil [89].

In light of the above, it is reasonable to state that Cr prefers binding to Fe NPs more than it does to soil, and thus may illustrates the potential of Fe NPs as a remediation material of soil against organic and

inorganic pollutants. This issue was a subject of intensive research during the last decade [18],[20].

The XRD analysis of the sample of soil-Fe NPs after exposure to Cr(VI) ions shows the formation of iron oxides and iron oxyhydroxide, indicating that Fe NPs has undergone corrosion, a typical XRD diagram of soil-Fe NPs after exposure to Cr(VI) ions is given in Fig. 27. The corrosion reaction can help create sorption sites on the surface of Fe NPs for Cr(VI) ions, and can also release iron ions that can be absorbed by soil. The corrosion reaction of GT-Fe NPs also verified by contacting the material with Cr(VI) ions. As shown by the TEM image in Fig. 28, the corrosion reaction yields clusters of iron oxide materials.

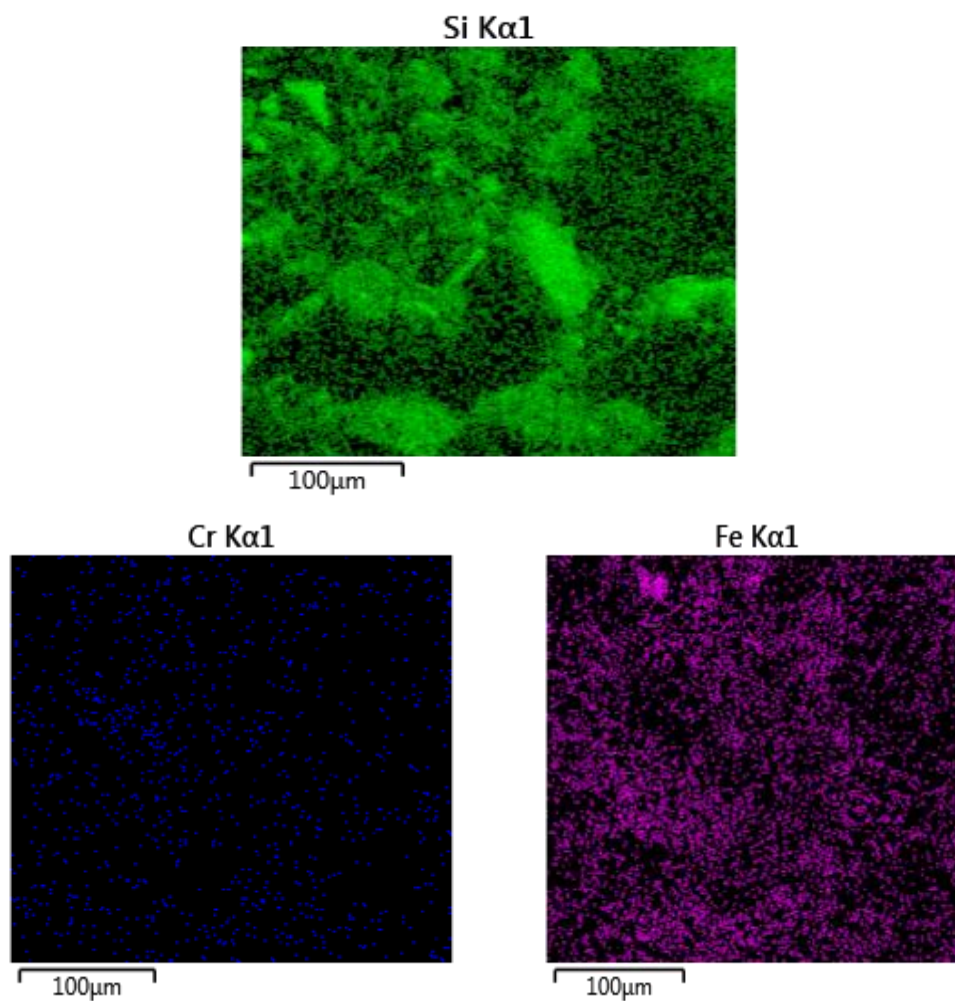


Figure 26 EDX mapping of a sample containing soil, Cr(VI) and GT-Fe NPs showing elemental maps for Fe, Si and Cr.

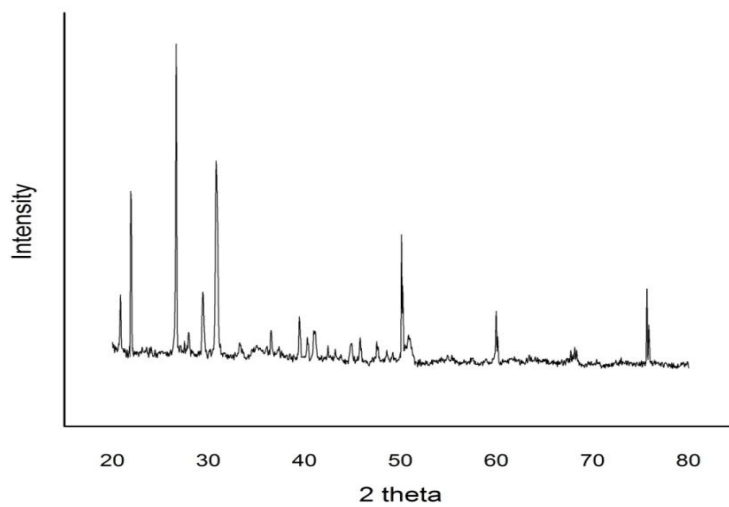


Figure 27 XRD pattern of a sample of Soil –GT-Fe NPs loaded with Cr (VI) ions.

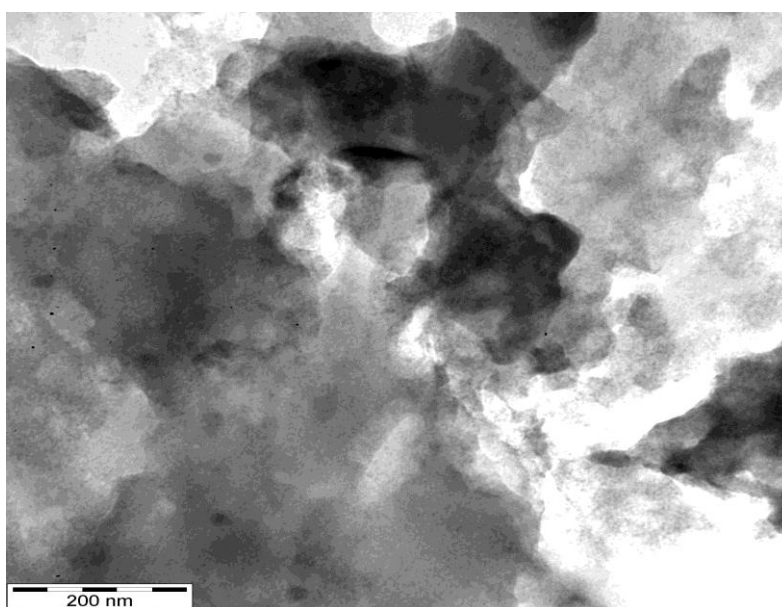


Figure 28 TEM image of GT-Fe NPs after the reaction with Cr(VI) ions.

3.3.2 Effect of Cr(VI) remediation from soil on Corn growth

In these experiments, soil was first mixed with Cr(VI) solutions, then it was mixed with nZVI, GT-Fe NPs, Z-nZVI, and zeolite. The quantities of each of the mixed materials are provided in Table 12. The table provides also the effect of the remediation process on the plant growth, expressed as percentage of plants that survived (the rate of survival). The percentage was calculated for each treatment by dividing the number of plants found (normal growth) by the total number of plants (total of 5 plants, each treatment was repeated five times).

The positive and negative controls stands for soil mixed with Cr(VI) and soil alone without added chemicals, respectively.

Figures 29 through 32 give some pictures for different plants showing different progress in their growth.



Figure 29 Some plants which didn't grow.



Figure 30 Some plants which grew normally.



Figure 31, Figure 32 Corn cobs that appeared in plants with normal growth at the end of the planting cycle.

Table 12 Summary of the quantities of Cr and remediating substances mixed with soil, and the effect of the process on plant progress through two months of planting.

		% Rate of survival	% Plant not found
1	positive control (soil + Cr (VI))	20	80
2	negative control (only soil)	100	0
3	zeolite 0.1 mg / Kg + Cr (VI) 200 mg / Kg	60	40
4	zeolite-nZVI 0.2 mg / Kg + Cr (VI) 200 mg / Kg	80	20
5	nZVI 0.1 mg / Kg + Cr (VI) 200 mg / Kg	60	40
6	GT-Fe 0.1 mg / Kg + Cr (VI) 200 mg / Kg	40	60
7	GT-Fe 1 mg / Kg + Cr (VI) 200 mg / Kg	0	100
8	zeolite 0.1 mg / Kg	40	60
9	zeolite-nZVI 0.2 mg / Kg	60	40
10	nZVI 0.1 mg / Kg	100	0
11	GT-Fe 0.1 mg / Kg	100	0
12	GT-Fe 1 mg / Kg	80	20

Based on the observed plant growth, the following conclusions can be drawn:

- a. When no Cr or Fe material was added to the soil, the plant was normal, 100% all the plants grew normally.
- b. When only Cr was added, only 20% of the plants grew. The fact that a single plant survived out of five suggests that Cr caused toxicity to the plants.
- c. Addition of nZVI (0.1 mg/Kg) to soil contaminated with Cr enhanced the plant growth, as the rate of survival was 60%, higher than 20% for Cr alone. This has happened by virtue of reducing the Cr concentration in soil as a result of sorption on nZVI.
- d. When GT-Fe NPs (0.1 mg/Kg) was added to Cr-contaminated soil, the rate of survival increased to 40%. This confirms that GT-Fe NPs contributed to reducing the soil contamination but it was not as effective as nZVI in doing so. When the GT-Fe concentration was increased to (1.0 mg/Kg), the rate of survival was found to increase to 60%, confirming the remediation effect of GT-Fe NPs.

- e. When the Cr-contaminated soil was mixed with Z-nZVI, the rate of survival was 80%, higher than the 60% for nZVI alone. A possible explanation of this comes from the effect of the addition of zeolite to nano iron, as zeolite addition was observed to decrease the aggregation of nano iron and so increase its efficiency in Cr removal. Another possible explanation could be that the zeolite material acted as a scavenger of Cr by virtue of its large surface area.
- f. Upon addition of zeolite to Cr-contaminated soil, the rate of survival was 60%.

The final result might lead to the conclusion that zeolite can be as effective as nZVI in soil remediation, and better than GT-Fe NPs. However, this approach ignores any diverse effects of these remediation materials on the soil free of Cr contamination.

In order to assess if the remediation materials have adverse effects on uncontaminated soil, each was added to soil and their effects on plant growth was observed. The obtained results can be summarized as follows:

- a. The addition of zeolite to the soil resulted in only 40% survival of plants, indicating that zeolite can harm the soil fertility. The reason for this could be holding ions and nutrients necessary for the plant growth inside the channels of zeolite structure.
- b. When nZVI was added to soil, the plant growth was normal, 100% of plants grew unaffected, indicating no negative effect of this material at the applied dose on soil fertility and plant nutrition.
- c. The addition of Z-nZVI to soil lead to 60% plant survival, confirming the diverse effect of zeolite on the plant growth.
- d. When GT-Fe NPs (0.1 mg/Kg) were added to soil, no negative effect was noticed on the plant growth as all the plants grew normally, suggesting that this dose of GT-Fe is not harmful to the plants. When the GT-Fe NPs concentration increased from 0.1 to 1.0 mg/Kg, some inhibition in the plant growth was noticed and the rate of survival decreased from 100% to 80%. This indicates that high concentration of Fe NPs can be harmful to the corn plants.

As a further assessment, the soil samples before and after planting were analyzed using ICP-OES for their Cr and Fe contents. The detailed ICP analysis results for Fe and Cr found in appendix B, and a summary of the results is provided in Tables 13 and 14. As the tables show, the average concentrations were calculated for the five replicates of each treatment, at the beginning of the planting (before) and after two months of planting (after).

Table 13 Summary of the ICP-OES analysis results for Fe

Fe	Avg. Before (mg/L)	Avg. After (mg/L)	Before – After (mg/L)
positive control	15132.2	5673.3	9458.9
negative control	12900.8	6111.0	6789.7
zeolite 0.1 mg / Kg + Cr (VI) 200 mg / Kg	16009.7	6753.9	9255.8
zeolite-nZVI 0.2 mg / Kg + Cr (VI) 200 mg / Kg	15222.7	5956.2	9266.5
nZVI 0.1 mg / Kg + Cr (VI) 200 mg / Kg	15334.5	5404.5	9930.0
GT-Fe 0.1 mg / Kg + Cr (VI) 200 mg / Kg	15797.8	6180.8	9617.1
GT-Fe 1 mg / Kg + Cr (VI) 200 mg / Kg	15432.7	5729.6	9703.1
zeolite 0.1 mg / Kg	15107.3	3009.7	12097.6
zeolite-nZVI 0.2 mg / Kg	14690.3	2770.2	11920.1
nZVI 0.1 mg / Kg	13880.9	2943.6	10937.3
GT-Fe 0.1 mg / Kg	15104.8	2896.6	12208.3
GT-Fe 1 mg / Kg	14168.6	2741.8	11426.8

Table 14 Summary of the ICP-OES analysis results for Cr

Cr	Avg. Before (mg/L)	Avg. After (mg/L)	Before – After (mg/L)
positive control	330.2	71.4	258.8
negative control	21.6	12.1	9.5
zeolite 0.1 mg / Kg + Cr (VI) 200 mg / Kg	240.7	85.2	155.5
zeolite-nZVI 0.2 mg / Kg + Cr (VI) 200 mg / Kg	290.0	73.2	216.8
nZVI 0.1 mg / Kg + Cr (VI) 200 mg / Kg	244.8	63.7	181.2
GT-Fe 0.1 mg / Kg + Cr (VI) 200 mg / Kg	249.2	73.6	175.6
GT-Fe 1 mg / Kg + Cr (VI) 200 mg / Kg	321.7	81.1	240.6
zeolite 0.1 mg / Kg	27.9	6.1	21.8
zeolite-nZVI 0.2 mg / Kg	23.9	4.5	19.4
nZVI 0.1 mg / Kg	21.2	4.7	16.5
GT-Fe 0.1 mg / Kg	21.6	4.7	16.9
GT-Fe 1 mg / Kg	20.5	4.1	16.3

In order to analyze the ICP results, as an attempt to relate them with the plant growth and progress, the differences between the chromium and iron concentrations were calculated as follows:

$$\Delta = \text{Concentration before} - \text{Concentration after ... (5)}$$

The depletion in Cr can occur in two ways; fixation by nano iron materials, and/or accumulation in the plant itself as reported in another study [90].

Table 15 shows the ICP analysis results (Δ values) for Cr in a descending order for samples to which Cr was added.

Table 16 shows the Δ values calculated in the same way for Fe in a descending order.

Table 15 The Δ values obtained from the ICP analysis for Cr(VI) in a descending order

(Δ = **Concentration before** – **Concentration after**, at the beginning of the planting (before), after two months of planting (after)).

Cr	Δ	
1	258.8	positive control (soil + Cr 200 mg / Kg)
7	240.6	GT-Fe 1.0 mg / Kg + Cr (VI) 200 mg / Kg
4	216.8	zeolite-nZVI 0.2 mg / Kg + Cr (VI) 200 mg / Kg
5	181.2	nZVI 0.1 mg / Kg + Cr (VI) 200 mg / Kg
6	175.6	GT-Fe 0.1 mg / Kg + Cr (VI) 200 mg / Kg
3	155.5	zeolite 0.1 mg / Kg + Cr (VI) 200 mg / Kg
8	21.8	zeolite 0.1 mg / Kg
9	19.4	zeolite-nZVI 0.2 mg / Kg
11	16.9	GT-Fe 0.1 mg / Kg
10	16.5	nZVI 0.1 mg / Kg
12	16.3	GT-Fe 1.0 mg / Kg
2	9.5	negative control

Table 16 The Δ values obtained from the ICP-OES analysis for Fe in a descending order

(Δ = **Concentration before** – **Concentration after**, at the beginning of the planting (before), after two months of planting (after)).

Fe	Δ	
11	12208.3	GT-Fe 0.1 mg / Kg
8	12097.6	zeolite 0.1 mg / Kg
9	11920.1	zeolite-nZVI 0.2 mg / Kg
12	11426.8	GT-Fe 1.0 mg / Kg
10	10937.3	nZVI 0.1 mg / Kg
5	9930.0	nZVI 0.1 mg / Kg + Cr (VI) 200 mg / Kg
7	9703.1	GT-Fe 1.0 mg / Kg + Cr (VI) 200 mg / Kg
6	9617.1	GT-Fe 0.1 mg / Kg + Cr (VI) 200 mg / Kg
1	9458.9	positive control (soil + Cr (VI) 200 mg / Kg)
4	9266.5	zeolite-nZVI 0.2 mg / Kg + Cr (VI) 200 mg / Kg
3	9255.8	zeolite 0.1 mg / Kg + Cr (VI) 200 mg / Kg
2	6789.7	negative control (only soil)

From the results in Tables 13 - 16, the following conclusions arise:

- a. The soil contained a relatively high Fe concentration as evident from the values in Table 13 for the soil samples to which no Fe nanomaterial was added (samples 1,2,8). The iron content was also detected by the EDX and XRF analysis of the soil.
- b. Upon addition of Fe nanomaterials, the Fe content of the soil showed some increase, which is in line with the limited amounts of added nano iron materials.
- c. In all cases there is a depletion of Cr and Fe elements. This is a strong indication that both elements are absorbed by the plant.
- d. As Table 15 shows, the highest Δ value for Cr is observed for the positive control to which no nano iron or zeolite material was added, hence it is logical to assume that Cr in this case was removed by accumulation into the plant, in line with previous studies [90].
- e. When nano iron materials are added to soil, the observed amount of depleted Cr is seen to decrease. This could be indicative that some Cr was immobilized on the nano iron materials and migrated into the soil, and/or the discrepancies in the results could be arising from sampling errors.

- f. Assuming that the smaller value of depleted Cr is due to immobilization by nano-iron materials, it can be seen that supported nano iron Z-nZVI is more efficient than nZVI alone as it showed a higher Δ value. This matches the observation in the plant progress part.
- g. It can be noticed that the lowest Δ value of Cr is observed for the negative control sample, here, no Cr or remediation substances were added to the soil.
- h. The depression of iron amount can be assumed to arise from the plant need for it as a nutrient. Plants require Fe to complete their life cycle. The importance of Fe is due to the existence of two stable, inter-convertible forms of this metal, which take part in fundamental processes involving electron transfer reactions, including respiration and photosynthesis [45].

3.4 Effect of iron nanoparticles on bacteria growth

In the following sections, the results of bacteria treatment with different Fe NP samples at different concentrations are presented in a descending order, with the highest bacterial growth being in the bottom. In the relevant experiments, the effect of Fe NPs on 4 bacteria types which are abundant in soil was examined. These bacteria types

are two gram positive bacteria (*Staphylococcus aureus* and *Bacillus subtilis*) and two are gram negative (*Klebsiella pneumonia* and *Escherichia coli*). The Fe NP samples which were tested were nZVI, GT-Fe, both in two different concentrations, in addition to Cr(VI) solution, and Cr(VI) mixed with Fe NPs.

The control sample (empty) in all experiments was bacteria alone without any added chemicals.

3.4.1 *Staphylococcus aureus*

The order of action of the tested solutions against this bacteria is shown in Fig. 33.

Based on the obtained results and trend for bacterial growth and inhibition, the following comments can be written:

1. The small concentration of Cr(VI) solution (10 mg/l) have a small negative effect on bacterial growth.
2. GT-Fe NPs inhibit the growth of bacteria to the same extent regardless of its concentration (GT-Fe 10 and GT-Fe 50 gave the same result).

3. nZVI inhibits the bacterial growth more than GT-Fe NPs, the higher the nZVI concentration, the higher the inhibition (nZVI 50 > nZVI 10).
4. The inhibition made by Cr + nZVI was higher than nZVI alone and Cr alone (Cr + nZVI > nZVI 50 > Cr 100), this may confirm that Cr(VI) has an adverse effect on the bacteria that adds to the adverse effect of nZVI.

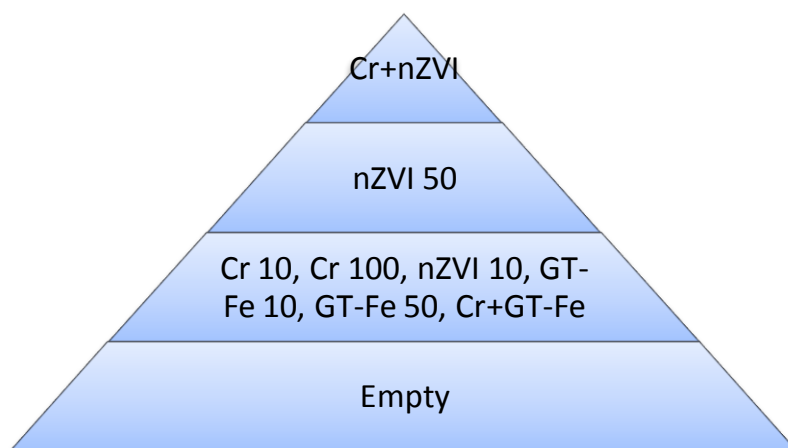


Figure 33 Inhibition of *S. aureus* bacterial growth in a descending order

nZVI 50 > GT-Fe 50 ~ GT-Fe 10 ~ nZVI 10 > Empty

3.4.2 *Klebsiella pneumonia*

Based on the results, shown in Fig. 34, the following comments can be written:

1. Cr(VI) solution at small concentration (10 mg/l) has no effect on bacterial growth, when the concentration increased to (100 mg/l), a small inhibition in the growth was observed.
2. Higher concentrations of Fe NPs (nZVI 50, GT-Fe 50) have higher negative effect on the bacteria growth than small concentrations (GT-Fe 10, nZVI 10).
3. nZVI 50 has a higher inhibition than GT-Fe 50.
4. Both of Cr + GT-Fe and Cr + nZVI results are almost the same as GT-Fe 50. This may be because Cr alone has a small effect on the bacteria growth.

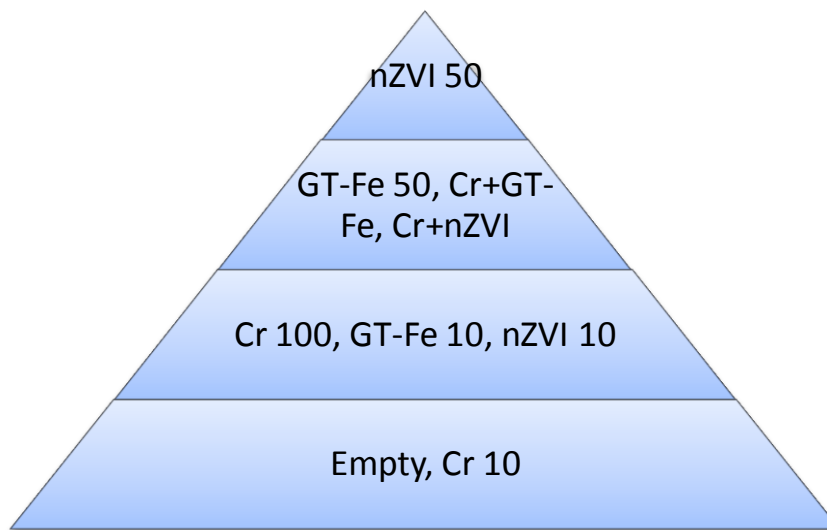


Figure 34 Inhibition of *K. Pneumonia* bacterial growth by various solutions in a descending order

$nZVI\ 50 > GT-Fe\ 50 > GT-Fe\ 10 \sim nZVI\ 10 > Empty$

3.4.3 *Bacillus subtilis*

According to the results, which are summarized in Fig. 35, the followings can be concluded:

1. Cr(VI) solution has no effect on bacterial growth on either concentrations.
2. GT-Fe in general is less toxic to *B. subtilis* than nZVI.
3. GT-Fe 50 and Cr + GT-Fe, nZVI 50 and Cr + nZVI, have the same results, and this seems to confirm that Cr alone has no effect on bacteria.

4. GT-Fe NPs have the same results on both concentrations, but for nZVI, nZVI 50 have a more negative effect on the bacteria growth than nZVI 10.

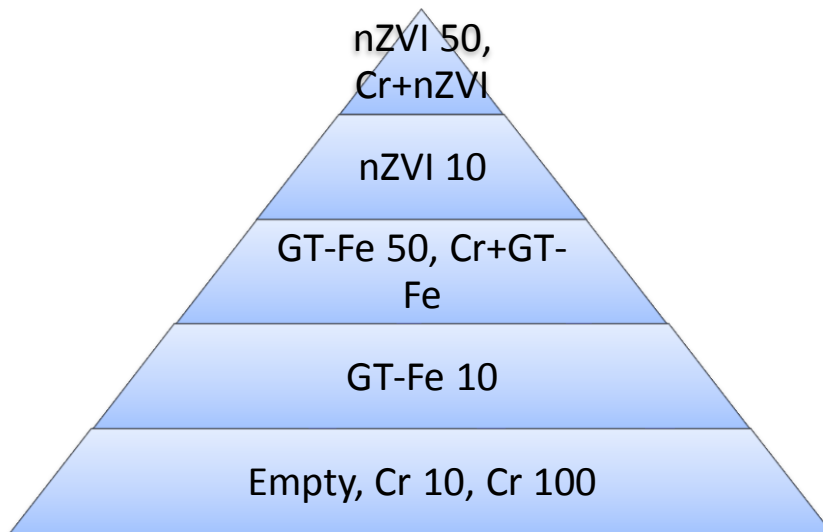


Figure 35 Inhibition of *B. Subtilis* bacterial growth by different solutions in a descending order

nZVI 50 > nZVI 10 > GT-Fe 50~GT-Fe 10 > Empty

3.4.4 *Escherichia coli*

Fig. 36 suggests that:

1. Small concentrations of Fe NPs (nZVI 10, GT-Fe 10) have no effect on this bacteria.

- Higher concentration of Fe NPs have a negative effect on the growth of bacteria, with GT-Fe 50 having the higher inhibition than nZVI 50.
- The effect of Cr(VI) is not very clear, but as the effects of Cr + GT-Fe and Cr + nZVI are higher than GT-Fe and nZVI respectively, it can be predicted that Cr alone has its own negative effect on bacteria growth.

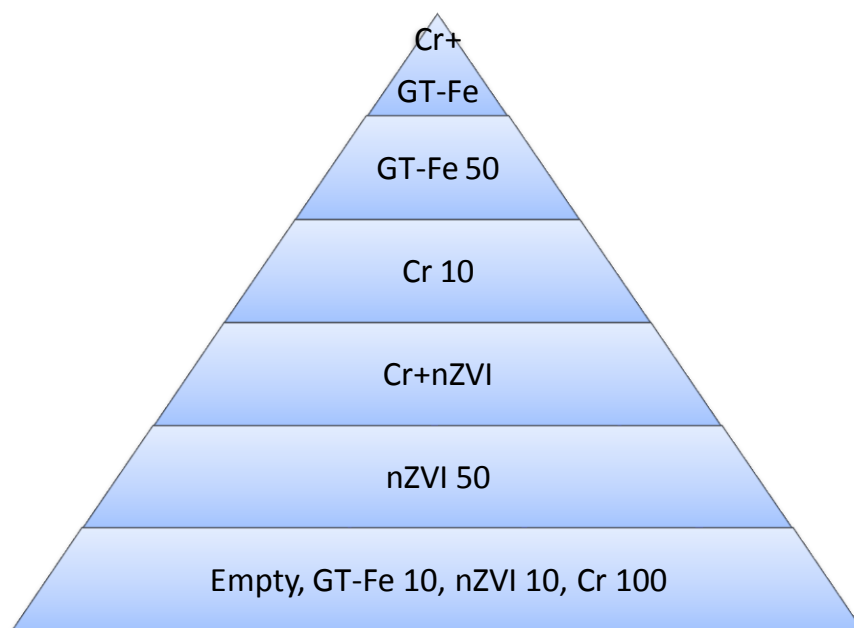


Figure 36 Inhibition of *E. coli* bacterial growth in a descending order

GT-Fe 50 > nZVI 50 > GT-Fe 10~nZVI 10~Empty

Based on the collective results of the tested bacteria the following conclusions can be made:

- i. Cr(VI) solutions have little effect on the tested bacteria types at low concentrations, and the detrimental effect is more obvious at higher concentrations. This seems to confirm the data reported in literature which suggest that Cr(VI) can cause shifts in the composition of soil microbial populations, and has detrimental effects on microbial cell metabolism at high concentrations [9].
- ii. nZVI (and Cr-nZVI) demonstrated the highest detrimental effect on all the bacteria types.
- iii. GT-Fe NPs have less detrimental effects than nZVI. This might be due to the fact that the organic groups coming from green tea occupies an important portion of the nanoparticles and thus reduces the Fe content in the nanoparticle.

The detrimental effects of various types of nanoparticles on bacteria types were reported in literature. For examples, Ag, Cu, MgO, ZnO, and TiO₂ NPs have been used to inactivate various biological agents including *B. subtilis* [16]. Both Ag and Cu nanoparticles inactivated *B. subtilis* and *Escherichia coli*, and *B. subtilis* was shown more

susceptible to the treatment. Also, it was found that the inactivation is depended on the concentrations of nanoparticles used [91].

It should be mentioned, however, that the reports on toxicities of metal and metal oxide NPs can be contradictory [16]. For example, some results show a lack of toxicity of nZVI on the cells of the Gram negative strain tested (*K. planticola*), even at the higher concentrations (10 mg/ml) after 24 h of exposure. In contrast, an inhibitory effect by the nanomaterial was observed on the Gram positive strain (*B. nealsonii*) [34]. nZVI particles were also reported to inactivate gram-negative *E. coli* [57].

Moreover, in a previous study, green-synthesized iron nanoparticles were reported to show good antibacterial activity against *Escherichia coli* and *Staphylococcus aureus* [26]. In other study, Fe₂O₃ NPs showed no significant antibacterial activities against *Escherichia coli* [54].

The size of nanoparticles can affect their antimicrobial activities [91]. Depending on synthesis methods for nZVI, and solution chemistries, different shell compositions such as FeO, maghemite (γ -

Fe₂O₃)/partially oxidized magnetite could be formed. The observed coating of iron oxides on bacterial membranes could block porins in the outer membrane of gram-negative, preventing their uptake of nutrients. For Gram positive bacteria, lipoteichoic acid, a component of the cell wall, might have formed a chelating complex with nZVI. Also, the anionic structures like in *B. subtilis* walls promote ferric hydroxide formation [92].

To conclude, it is evident from this study that Fe NPs demonstrate serious inhibition effects on the studied bacteria types. This leads to the result that treating the soil with iron nanoparticles will seriously affect its bacteria content. The extent of the effect will depend significantly on the applied concentration.

4. Conclusions

Both of nZVI and Z-nZVI materials are very effective in Cr(VI) removal, for nZVI, equilibrium of Cr(VI) removal is approached in about one hour of contact between liquid and solid phases. For Z-nZVI, the process was slower and more than four hours were required to attain equilibrium. The data of Z-nZVI obeyed pseudo first order kinetics, with k_1 (rate constant) calculated as $3.4 * 10^{-3} \pm 0.2 * 10^{-3} \text{ min}^{-1}$, and Q_{max} (maximum sorbable amount) found as $24 \pm 1 \text{ mg/g}$.

The removal of Cr(VI) is high over a wide range of pH values although the removal decrease in the alkaline medium. Generally, the removal of Cr(VI) by Z-nZVI is more pH-dependent than that of nZVI.

Cr signals from the EDX mapping analysis appear to be associated with the Fe signals, not with Si, indicating that Cr ions favors binding to iron nanoparticles more than to soil particles.

XRD analysis of the sample of soil-Fe NPs after exposure to Cr(VI) ions shows formation of iron oxides and iron oxyhydroxide, indicating that Fe NPs has undergone corrosion.

No negative effect of nZVI and GT-Fe on Corn growth at the lower applied dose (0.1 mg/Kg) on soil fertility and plant nutrition was observed, however, high concentrations of Fe NPs can be harmful to the corn plants. Cr and Fe elements are highly depleted from soil, most probably through uptake by plants.

Cr(VI) solutions at low levels had slight effect on the tested bacteria types. GT-Fe NPs negative impact was lower than nZVI.

Similar studies are required to test the effect of Fe NPs on other plants and optimize the amount of this material such that remediation of pollutants can be achieved without harming the soil and plants.

5. References

- (1) Mohan, D.; Pittman, C. U. Activated Carbons and Low Cost Adsorbents for Remediation of Tri- and Hexavalent Chromium from Water. *J. Hazard. Mater.* **2006**, *137* (2), 762–811.
- (2) Loska, K.; Wiechulla, D.; Korus, I. Metal Contamination of Farming Soils Affected by Industry. *Environ. Int.* **2004**, *30* (2), 159–165.
- (3) Li, X.; Liu, L.; Wang, Y.; Luo, G.; Chen, X.; Yang, X.; Hall, M. H. P.; Guo, R.; Wang, H.; Cui, J.; et al. Heavy Metal Contamination of Urban Soil in an Old Industrial City (Shenyang) in Northeast China. *Geoderma* **2013**, *192* (1), 50–58.
- (4) Yaylali-Abanuz, G. Heavy Metal Contamination of Surface Soil around Gebze Industrial Area, Turkey. *Microchem. J.* **2011**, *99* (1), 82–92.
- (5) Kumar Sharma, R.; Agrawal, M.; Marshall, F. Heavy Metal Contamination of Soil and Vegetables in Suburban Areas of Varanasi, India. *Ecotoxicol. Environ. Saf.* **2007**, *66* (2), 258–266.
- (6) O'Carroll, D.; Sleep, B.; Krol, M.; Boparai, H.; Kocur, C. Nanoscale Zero Valent Iron and Bimetallic Particles for

- Contaminated Site Remediation. *Adv. Water Resour.* **2013**, *51*, 104–122.
- (7) Zhong, L.; Yang, J. Reduction of Cr(VI) by Malic Acid in Aqueous Fe-Rich Soil Suspensions. *Chemosphere* **2012**, *86* (10), 973–978.
- (8) Economou-Eliopoulos, M.; Antivachi, D.; Vasilatos, C.; Megremi, I. Evaluation of the Cr(VI) and Other Toxic Element Contamination and Their Potential Sources: The Case of the Thiva Basin (Greece). *Geosci. Front.* **2012**, *3* (4), 523–539.
- (9) Huang, S. H.; Peng, B.; Yang, Z. H.; Chai, L. Y.; Zhou, L. C. Chromium Accumulation, Microorganism Population and Enzyme Activities in Soils around Chromium-Containing Slag Heap of Steel Alloy Factory. *Trans. Nonferrous Met. Soc. China (English Ed.)* **2009**, *19* (1), 241–248.
- (10) Shanker, A. K.; Cervantes, C.; Loza-Tavera, H.; Avudainayagam, S. Chromium Toxicity in Plants. *Environ. Int.* **2005**, *31* (5), 739–753.
- (11) Zhang, J.; Xu, Y.; Li, W.; Zhou, J.; Zhao, J.; Qian, G.; Xu, Z. P. Enhanced Remediation of Cr(VI)-Contaminated Soil by

- Incorporating a Calcined-Hydrotalcite-Based Permeable Reactive Barrier with Electrokinetics. *J. Hazard. Mater.* **2012**, 239-240, 128–134.
- (12) Mijangos, I.; Pérez, R.; Albizu, I.; Garbisu, C. Effects of Fertilization and Tillage on Soil Biological Parameters. *Enzyme Microb. Technol.* **2006**, 40 (1), 100–106.
- (13) Beukes, J. P.; Pienaar, J. J.; Lachmann, G. The Reduction of Hexavalent Chromium by Sulphite in Wastewater - An Explanation of the Observed Reactivity Pattern. *Water SA* **2000**, 26 (3), 393–395.
- (14) Liu, T.; Wang, Z.-L.; Zhao, L.; Yang, X. Enhanced chitosan/Fe⁰-Nanoparticles Beads for Hexavalent Chromium Removal from Wastewater. *Chem. Eng. J.* **2012**, 189-190, 196–202.
- (15) Cullen, L. G.; Tilston, E. L.; Mitchell, G. R.; Collins, C. D.; Shaw, L. J. Assessing the Impact of Nano- and Micro-Scale Zerovalent Iron Particles on Soil Microbial Activities: Particle Reactivity Interferes with Assay Conditions and Interpretation of Genuine Microbial Effects. *Chemosphere* **2011**, 82 (11), 1675–

1682.

- (16) Dinesh, R.; Anandaraj, M.; Srinivasan, V.; Hamza, S. Engineered Nanoparticles in the Soil and Their Potential Implications to Microbial Activity. *Geoderma* **2012**, *173-174*, 19–27.
- (17) Crane, R. a.; Scott, T. B. Nanoscale Zero-Valent Iron: Future Prospects for an Emerging Water Treatment Technology. *J. Hazard. Mater.* **2012**, *211-212*, 112–125.
- (18) Cundy, A. B.; Hopkinson, L.; Whitby, R. L. D. Use of Iron-Based Technologies in Contaminated Land and Groundwater Remediation: A Review. *Sci. Total Environ.* **2008**, *400* (1-3), 42–51.
- (19) Liu, H.; Chen, T.; Zou, X.; Xie, Q.; Qing, C.; Chen, D.; Frost, R. L. Removal of Phosphorus Using NZVI Derived from Reducing Natural Goethite. *Chem. Eng. J.* **2013**, *234*, 80–87.
- (20) Machado, S.; Stawiński, W.; Slonina, P.; Pinto, a. R.; Grosso, J. P.; Nouws, H. P. a; Albergaria, J. T.; Delerue-Matos, C. Application of Green Zero-Valent Iron Nanoparticles to the Remediation of Soils Contaminated with Ibuprofen. *Sci. Total*

Environ. **2013**, 461-462, 323–329.

- (21) Chen, J.; Qiu, X.; Fang, Z.; Yang, M.; Pokeung, T.; Gu, F.; Cheng, W.; Lan, B. Removal Mechanism of Antibiotic Metronidazole from Aquatic Solutions by Using Nanoscale Zero-Valent Iron Particles. *Chem. Eng. J.* **2012**, 181-182, 113–119.
- (22) Unal Yesiller, S.; Eroğlu, a. E.; Shahwan, T. Removal of Aqueous Rare Earth Elements (REEs) Using Nano-Iron Based Materials. *J. Ind. Eng. Chem.* **2013**, 19 (3), 898–907.
- (23) Efecan, N.; Shahwan, T.; Eroğlu, A. E.; Lieberwirth, I. Characterization of the Uptake of Aqueous Ni²⁺ Ions on Nanoparticles of Zero-Valent Iron (nZVI). *Desalination* **2009**, 249 (3), 1048–1054.
- (24) Li, Y.; Li, T.; Jin, Z. Stabilization of Fe⁰ Nanoparticles with Silica Fume for Enhanced Transport and Remediation of Hexavalent Chromium in Water and Soil. *J. Environ. Sci.* **2011**, 23 (7), 1211–1218.
- (25) Huang, L.; Weng, X.; Chen, Z.; Megharaj, M.; Naidu, R. Synthesis of Iron-Based Nanoparticles Using Oolong Tea

- Extract for the Degradation of Malachite Green. *Spectrochim. Acta - Part A Mol. Biomol. Spectrosc.* **2014**, *117*, 801–804.
- (26) Naseem, T.; Farrukh, M. A. Antibacterial Activity of Green Synthesis of Iron Nanoparticles Using Lawsonia Inermis and Gardenia Jasminoides Leaves Extract. *J. Chem.* **2015**, *2015* (Article ID 912342, 7 pages), doi:10.1155/2015/912342.
- (27) Yan, W.; Herzing, A. a.; Kiely, C. J.; Zhang, W. X. Nanoscale Zero-Valent Iron (nZVI): Aspects of the Core-Shell Structure and Reactions with Inorganic Species in Water. *J. Contam. Hydrol.* **2010**, *118* (3-4), 96–104.
- (28) University, G. S. Table of Standard Electrode Potentials <http://hyperphysics.phy-astr.gsu.edu/hbase/tables/electpot.html> (accessed Aug 8, 2015).
- (29) Zhang, W.-X. Nanoscale Iron Particles for Environmental Remediation: An Overview. *J. Nanoparticle Res.* **2003**, *5*, 323–332.
- (30) Grieger, K. D.; Fjordbøge, A.; Hartmann, N. B.; Eriksson, E.; Bjerg, P. L.; Baun, A. Environmental Benefits and Risks of Zero-Valent Iron Nanoparticles (nZVI) for in Situ Remediation:

- Risk Mitigation or Trade-Off? *J. Contam. Hydrol.* **2010**, *118* (3-4), 165–183.
- (31) Du, J.; Lu, J.; Wu, Q.; Jing, C. Reduction and Immobilization of Chromate in Chromite Ore Processing Residue with Nanoscale Zero-Valent Iron. *J. Hazard. Mater.* **2012**, *215-216*, 152–158.
- (32) Araújo, R.; Castro, A. C. M.; Fiúza, A. The Use of Nanoparticles in Soil and Water Remediation Processes. *Mater. Today Proc.* **2015**, *2* (1), 315–320.
- (33) Fang, Z.; Qiu, X.; Huang, R.; Qiu, X.; Li, M. Removal of Chromium in Electroplating Wastewater by Nanoscale Zero-Valent Metal with Synergistic Effect of Reduction and Immobilization. *Desalination* **2011**, *280* (1-3), 224–231.
- (34) Fajardo, C.; Ortíz, L. T.; Rodríguez-Membibre, M. L.; Nande, M.; Lobo, M. C.; Martín, M. Assessing the Impact of Zero-Valent Iron (ZVI) Nanotechnology on Soil Microbial Structure and Functionality: A Molecular Approach. *Chemosphere* **2012**, *86* (8), 802–808.
- (35) Kumpiene, J.; Ore, S.; Renella, G.; Mench, M.; Lagerkvist, A.; Maurice, C. Assessment of Zerovalent Iron for Stabilization of

- Chromium, Copper, and Arsenic in Soil. *Environ. Pollut.* **2006**, *144* (1), 62–69.
- (36) Li, X.; Cao, J.; Zhang, W. Stoichiometry of Cr (VI) Immobilization Using Nanoscale Zerovalent Iron (nZVI): A Study with High-Resolution X-Ray Photoelectron Spectroscopy (HR-XPS). *Ind. Eng. Chem. Res.* **2008**, *47*, 2131–2139.
- (37) Qiu, X.; Fang, Z.; Yan, X.; Cheng, W.; Lin, K. Chemical Stability and Toxicity of Nanoscale Zero-Valent Iron in the Remediation of Chromium-Contaminated Watershed. *Chem. Eng. J.* **2013**, *220*, 61–66.
- (38) Li, Y.; Li, J.; Zhang, Y. Mechanism Insights into Enhanced Cr(VI) Removal Using Nanoscale Zerovalent Iron Supported on the Pillared Bentonite by Macroscopic and Spectroscopic Studies. *J. Hazard. Mater.* **2012**, *227-228*, 211–218.
- (39) Shi, L. N.; Lin, Y. M.; Zhang, X.; Chen, Z. L. Synthesis, Characterization and Kinetics of Bentonite Supported nZVI for the Removal of Cr(VI) from Aqueous Solution. *Chem. Eng. J.* **2011**, *171* (2), 612–617.
- (40) Lv, X.; Hu, Y.; Tang, J.; Sheng, T.; Jiang, G.; Xu, X. Effects of

Co-Existing Ions and Natural Organic Matter on Removal of Chromium (VI) from Aqueous Solution by Nanoscale Zero Valent Iron (nZVI)-Fe₃O₄ Nanocomposites. *Chem. Eng. J.* **2013**, *218*, 55–64.

- (41) Wang, Y.; Fang, Z.; Liang, B.; Tsang, E. P. Remediation of Hexavalent Chromium Contaminated Soil by Stabilized Nanoscale Zero-Valent Iron Prepared from Steel Pickling Waste Liquor. *Chem. Eng. J.* **2014**, *247*, 283–290.
- (42) Chrysochoou, M.; Johnston, C. P.; Dahal, G. A Comparative Evaluation of Hexavalent Chromium Treatment in Contaminated Soil by Calcium Polysulfide and Green-Tea Nanoscale Zero-Valent Iron. *J. Hazard. Mater.* **2012**, *201-202*, 33–42.
- (43) Qiu, X.; Fang, Z.; Yan, X.; Gu, F.; Jiang, F. Emergency Remediation of Simulated Chromium (VI)-Polluted River by Nanoscale Zero-Valent Iron: Laboratory Study and Numerical Simulation. *Chem. Eng. J.* **2012**, *193-194*, 358–365.
- (44) Sheykhbaglou, R.; Sedghi, M. Effects of Nano-Iron Oxide Particles on Agronomic Traits of Soybean. *Not. Sci. Biol.* **2010**, *2* (2), 112–113.

- (45) De Nisi, P.; Vigani, G.; Dell'Orto, M.; Zocchi, G. Application of the Split Root Technique to Study Iron Uptake in Cucumber Plants. *Plant Physiol. Biochem.* **2012**, *57*, 168–174.
- (46) Ma, X.; Geiser-lee, J.; Deng, Y.; Kolmakov, A. Science of the Total Environment Interactions between Engineered Nanoparticles (ENPs) and Plants : Phytotoxicity , Uptake and Accumulation. *Sci. Total Environ.* **2010**, *408* (16), 3053–3061.
- (47) Prasad, M. N. V. deficiency and toxicity symptoms Contents : <http://nsdl.niscair.res.in/jspui/bitstream/123456789/340/1/Formatted - Revised Plant mineral nutrition.pdf> (accessed Jan 3, 2016).
- (48) Quik, J. T. K.; Vonk, J. A.; Hansen, S. F.; Baun, A.; Van De Meent, D. How to Assess Exposure of Aquatic Organisms to Manufactured Nanoparticles? *Environ. Int.* **2011**, *37* (6), 1068–1077.
- (49) Yin, K.; Lo, I. M. C.; Dong, H.; Rao, P.; Mak, M. S. H. Lab-Scale Simulation of the Fate and Transport of Nano Zero-Valent Iron in Subsurface Environments: Aggregation, Sedimentation, and Contaminant Desorption. *J. Hazard. Mater.* **2012**, *227-228*, 118–125.

- (50) Lin, D.; Xing, B. Phytotoxicity of Nanoparticles: Inhibition of Seed Germination and Root Growth. *Environ. Pollut.* **2007**, *150* (2), 243–250.
- (51) Ma, X.; Gurung, A.; Deng, Y. Phytotoxicity and Uptake of Nanoscale Zero-Valent Iron (nZVI) by Two Plant Species. *Sci. Total Environ.* **2013**, *443*, 844–849.
- (52) Kalantari, N. Evaluation of Toxicity of Iron , Chromium and Cadmium on Bacillus Cereus Growth. *Iran. J. Basic Med. Sci.* **2008**, *10* (4), 222–228.
- (53) Serrano, a.; Tejada, M.; Gallego, M.; Gonzalez, J. L. Evaluation of Soil Biological Activity after a Diesel Fuel Spill. *Sci. Total Environ.* **2009**, *407* (13), 4056–4061.
- (54) Wang, Z.; Lee, Y.-H.; Wu, B.; Horst, A.; Kang, Y.; Tang, Y. J.; Chen, D.-R. Anti-Microbial Activities of Aerosolized Transition Metal Oxide Nanoparticles. *Chemosphere* **2010**, *80* (5), 525–529.
- (55) Qiu, X.; Fang, Z.; Yan, X.; Cheng, W.; Lin, K. Chemical Stability and Toxicity of Nanoscale Zero-Valent Iron in the Remediation of Chromium-Contaminated Watershed. *Chem.*

Eng. J. **2013**, 220, 61–66.

- (56) Chen, J.; Xiu, Z.; Lowry, G. V.; Alvarez, P. J. J. Effect of Natural Organic Matter on Toxicity and Reactivity of Nano-Scale Zero-Valent Iron. *Water Res.* **2011**, 45 (5), 1995–2001.
- (57) Auffan, M.; Achouak, W.; Rose, J.; Roncato, M. A.; Chanéac, C.; Waite, D. T.; Masion, A.; Woicik, J. C.; Wiesner, M. R.; Bottero, J. Y. Relation between the Redox State of Iron-Based Nanoparticles and Their Cytotoxicity toward Escherichia Coli. *Environ. Sci. Technol.* **2008**, 42 (17), 6730–6735.
- (58) Diao, M.; Yao, M. Use of Zero-Valent Iron Nanoparticles in Inactivating Microbes. *Water Res.* **2009**, 43 (20), 5243–5251.
- (59) El-Temsah, Y. S.; Joner, E. J. Ecotoxicological Effects on Earthworms of Fresh and Aged Nano-Sized Zero-Valent Iron (nZVI) in Soil. *Chemosphere* **2012**, 89 (1), 76–82.
- (60) What is Staphylococcus Aureus <http://www.news-medical.net/health/What-is-Staphylococcus-Aureus.aspx>
(accessed Aug 5, 2015).
- (61) Staphylococcus aureus_ USA_300 - MicrobeWiki
https://microbewiki.kenyon.edu/index.php/Staphylococcus_aureus

us:_USA:300 (accessed Aug 5, 2015).

- (62) *Klebsiella pneumoniae* - Wikipedia, the free encyclopedia
https://en.wikipedia.org/wiki/Klebsiella_pneumoniae (accessed Aug 5, 2015).
- (63) *Bacillus subtilis* - MicrobeWiki
https://microbewiki.kenyon.edu/index.php/Bacillus_subtilis
(accessed Aug 5, 2015).
- (64) *Bacillus subtilis* - Wikipedia, the free encyclopedia
https://en.wikipedia.org/wiki/Bacillus_subtilis (accessed Aug 5, 2015).
- (65) General information of Oil palm.pdf
<http://www.cdc.gov/ecoli/general/index.html> (accessed Aug 5, 2015).
- (66) *Escherichia coli* - Wikipedia, the free encyclopedia
https://en.wikipedia.org/wiki/Escherichia_coli (accessed Aug 5, 2015).
- (67) Nairat, M.; Shahwan, T.; Erog, A. E.; Fuchs, H. Incorporation of Iron Nanoparticles into Clinoptilolite and Its Application for the Removal of Cationic and Anionic Dyes. *J. Ind. Eng. Chem.*

2015, 21, 1143–1151.

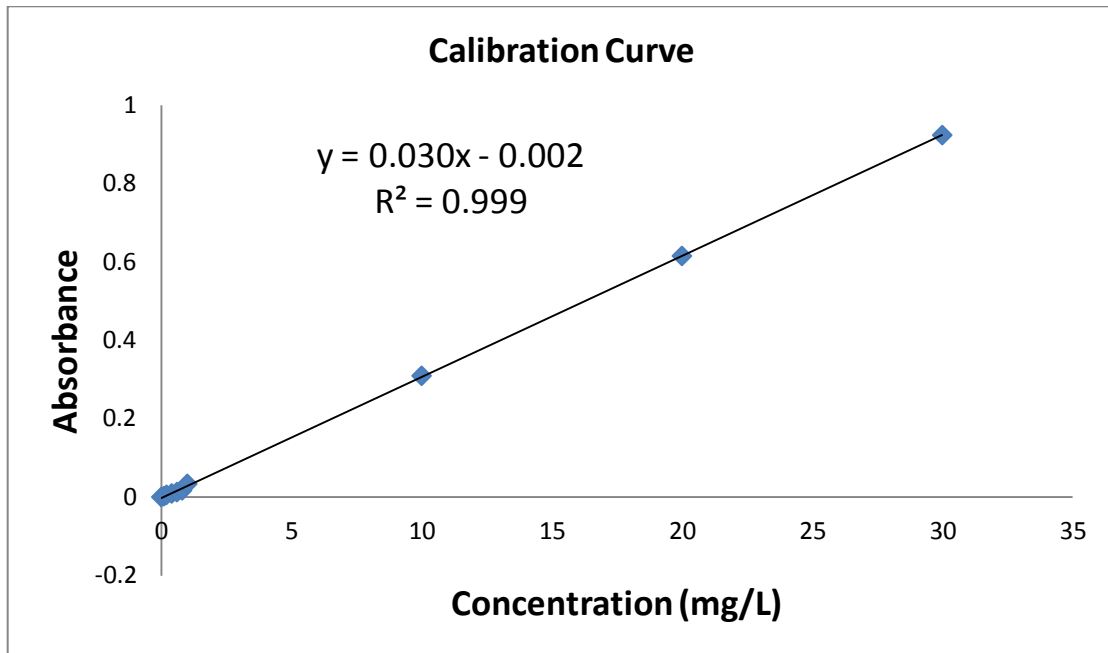
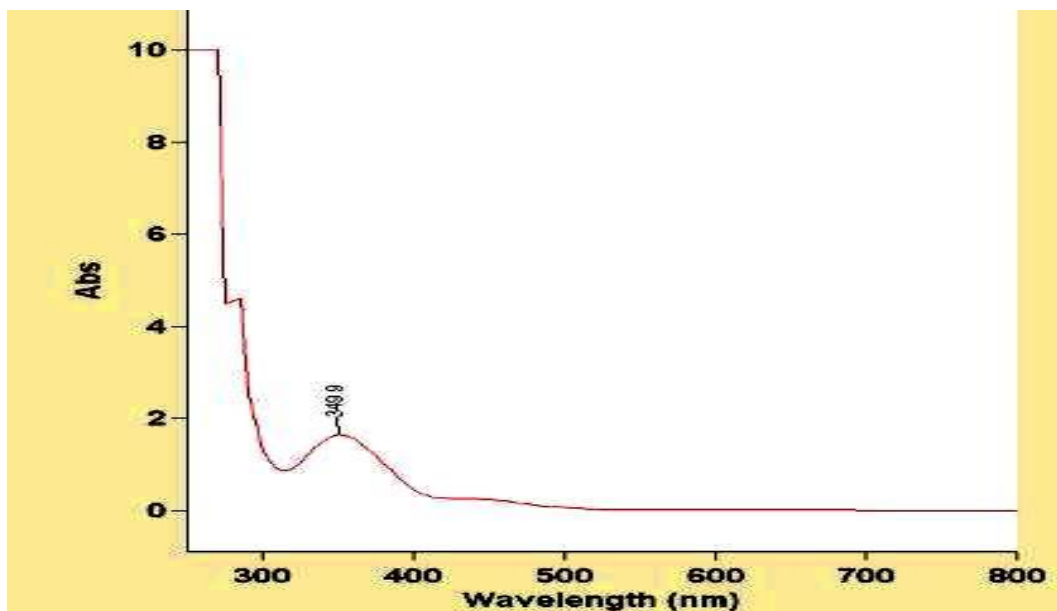
- (68) Nairat, M. Synthesis and Characterization of Nano-Iron Based Materials and Their Application for the Removal of Anionic and Cationic Dyes. Master Thesis in Applied Chemistry, Birzeit university, 2013.
- (69) Shahwan, T.; Sirriah, S. A.; Nairat, M.; Boyacı, E.; Ero, A. E.; Scott, T. B.; Hallam, K. R. Green Synthesis of Iron Nanoparticles and Their Application as a Fenton-like Catalyst for the Degradation of Aqueous Cationic and Anionic Dyes. *Chem. Eng. J.* **2011**, 172, 258–266.
- (70) Ju-Nam, Y.; Lead, J. R. Manufactured Nanoparticles: An Overview of Their Chemistry, Interactions and Potential Environmental Implications. *Sci. Total Environ.* **2008**, 400 (1-3), 396–414.
- (71) BET theory - Wikipedia, the free encyclopedia http://en.wikipedia.org/wiki/BET_theory (accessed Aug 3, 2015).
- (72) X-ray Diffraction (XRD) | XOS <http://www.xos.com/techniques/xrd/> (accessed Aug 3, 2015).

- (73) Swapp, S. Scanning Electron Microscopy (SEM)
http://serc.carleton.edu/research_education/geochemsheets/techniques/SEM.html (accessed Aug 3, 2015).
- (74) Intertek Group plc. Energy Dispersive X-Ray Analysis (EDX)
<http://www.intertek.com/analysis/microscopy/edx/> (accessed Aug 3, 2015).
- (75) Overview of XRF
http://archaeometry.missouri.edu/xrf_overview.html (accessed Aug 3, 2015).
- (76) Peralta-Videa, J. R.; Zhao, L.; Lopez-Moreno, M. L.; de la Rosa, G.; Hong, J.; Gardea-Torresdey, J. L. Nanomaterials and the Environment: A Review for the Biennium 2008-2010. *J. Hazard. Mater.* **2011**, *186* (1), 1–15.
- (77) Singh, R.; Misra, V.; Singh, R. P. Synthesis, Characterization and Role of Zero-Valent Iron Nanoparticle in Removal of Hexavalent Chromium from Chromium-Spiked Soil. *J. Nanoparticle Res.* **2011**, *13* (9), 4063–4073.
- (78) R Riley. Bragg's Law for X-Ray Crystal Diffraction. *production* **1970**, *5* (6), 371–372.

- (79) Singh, V.; Agrawal, H. M. Qualitative Soil Mineral Analysis by EDXRF, XRD and AAS Probes. *Radiat. Phys. Chem.* **2012**, *81* (12), 1796–1803.
- (80) Shahwan, T. Sorption Kinetics: Obtaining a Pseudo-Second Order Rate Equation Based on a Mass Balance Approach. *J. Environ. Chem. Eng.* **2014**, *2* (2), 1001–1006.
- (81) Shahwan, T. Lagergren Equation: Can Maximum Loading of Sorption Replace Equilibrium Loading? *Chem. Eng. Res. Des.* **2015**, *96*, 172–176.
- (82) Ramazanpour Esfahani, A.; Hojati, S.; Azimi, A.; Farzadian, M.; Khataee, A. Enhanced Hexavalent Chromium Removal from Aqueous Solution Using a Sepiolite-Stabilized Zero-Valent Iron Nanocomposite: Impact of Operational Parameters and Artificial Neural Network Modeling. *J. Taiwan Inst. Chem. Eng.* **2015**, *49*, 172–182.
- (83) Soil pH - Wikipedia, the free encyclopedia
http://en.wikipedia.org/wiki/Soil_pH#Determining_pH
(accessed Jan 3, 2016).
- (84) Mitra, P.; Sarkar, D.; Chakrabarti, S.; Dutta, B. K. Reduction of

- Hexa-Valent Chromium with Zero-Valent Iron: Batch Kinetic Studies and Rate Model. *Chem. Eng. J.* **2011**, *171* (1), 54–60.
- (85) Kumral, E. “Speciation of Chromium in Waters Via Sol-Gel Preconcentration Prior To Atomic Spectrometric Determination”. Master Degree in Chemistry, Izmir Institute of Technology, 2007.
- (86) Fendorf M.J. AU3 - Grossl, P. AU4 - Sparks, D.L., S. A.-E. Arsenate and Chromate Retention Mechanisms on Goethite. *Environ. Sci. Technol.* **1997**, *31* (2), 315–320.
- (87) Petala, E.; Dimos, K.; Douvalis, A.; Bakas, T.; Tucek, J. Nanoscale Zero-Valent Iron Supported on Mesoporous Silica : Characterization and Reactivity for Cr (VI) Removal from Aqueous Solution. *J. Hazard. Mater.* **2013**, *261*, 295–306.
- (88) Potentials, S. R. Standard Reduction Potential Table Standard Reduction Potential Table
<http://www.chemeddl.org/services/moodle/media/QBank/GenChem/Tables/EStandardTable.htm> (accessed Jul 23, 2015).
- (89) Fendorf, S. E. Surface Reactions of Chromium in Soils and Waters. *Geoderma* **1995**, *67* (1-2), 55–71.

- (90) Alhousani, M. Phytoremediation of Agricultural Land Polluted with Heavy Metals in Wadi Alsamin - Hebron-Palestine. Master Thesis in Environment and Water Sciences, Birzeit university, 2012.
- (91) Yoon, K. Y.; Hoon Byeon, J.; Park, J. H.; Hwang, J. Susceptibility Constants of Escherichia Coli and Bacillus Subtilis to Silver and Copper Nanoparticles. *Sci. Total Environ.* **2007**, 373 (2-3), 572–575.
- (92) Chen, Q.; Gao, M.; Li, J.; Shen, F.; Wu, Y.; Xu, Z.; Yao, M. Inactivation and Magnetic Separation of Bacteria from Liquid Suspensions Using Electrosprayed and Nonelectrosprayed nZVI Particles: Observations and Mechanisms. *Environ. Sci. Technol.* **2012**, 46 (4), 2360–2367.

APPENDIX A – λ_{\max} Scan & calibration curve for Cr (VI)**Figure A-1 Calibration curve****Figure A-2 Maximum wavelength scan for Cr (VI) ($\lambda_{\max} = 350 \text{ nm}$)**

APPENDIX B --- ICP-OES ANALYSIS RESULTS**NOTE : A1 – before, 2A1 – after.****Fe (mg/L)**

A1	14068.3	2A1	15508.3
A2	6611.8	2A2	16129.1
A3	14130.4	2A3	17836.9
A4	13958.5	2A4	15658.2
A5	13579.5	2A5	14553.9
A6	15099.9	2A6	14222.8
A7	13596.7	2A7	13752.5
A8	14184.7	2A8	14117.8
A9	13850.4	2A9	13138.5
A10	13373.1	2A10	13966.7
A11	12967.8	2A11	13737.1
A12	11744.3	2A12	12904.7

B1	13565.5	2B1	12414.3
B2	11384.5	2B2	13884.5
B3	13764.6	2B3	15406.3
B4	13755	2B4	13481.6
B5	14792.2	2B5	11999
B6	13928.8	2B6	16166.3
B7	14805.1	2B7	14226.4
B8	15443.2	2B8	437.85
B9	13121.7	2B9	169.1
B10	13978.7	2B10	139.91
B11	14043.3	2B11	184.51
B12	15361.7	2B12	176.97

C1	16127.9	2C1	144.83
C2	15586.7	2C2	295.3
C3	17093	2C3	157.46
C4	14795.8	2C4	268.49
C5	16794	2C5	105.39
C6	17160.5	2C6	95.17

C7	15108	2C7	293.04
C8	15761.2	2C8	171.5
C9	14466.6	2C9	251.91
C10	15969.7	2C10	204.26
C11	15626.2	2C11	144.4
C12	13772.9	2C12	218.17
D1	15954.6	2D1	166.72
D2	14165.8	2D2	120.8
D3	17010.7	2D3	159.47
D4	16204.2	2D4	153.54
D5	15268.3	2D5	110.83
D6	15916.7	2D6	172.39
D7	16637.2	2D7	159.02
D8	15506.7	2D8	114.96
D9	15758.1	2D9	101.03
D10	15079.9	2D10	153.26
D11	16566.8	2D11	146.62
D12	14560	2D12	147.82

E1	15944.6	2 E1	132.28
E2	16755.1	2 E2	125.5
E3	18050	2 E3	209.48
E4	17400	2 E4	219.39
E5	16238.3	2 E5	253.16
E6	16883.3	2 E6	247.25
E7	17016.7	2 E7	217.17
E8	14640.7	2 E8	206.39
E9	16254.6	2 E9	190.58
E10	11003	2 E10	253.99
E11	16320	2 E11	270.15
E12	15404.2	2 E12	261.24

Cr (mg/L)

A1	310.67	2A1	204.67
A2	15.47	2A2	32.95
A3	238.13	2A3	227.45
A4	352.16	2A4	185.18
A5	248.59	2A5	193.58
A6	261.41	2A6	173.7
A7	390.83	2A7	159.47
A8	30.78	2A8	30.46
A9	25	2A9	22.31
A10	23.53	2A10	23.67
A11	22.4	2A11	23.4
A12	19.95	2A12	20.65

B1	395.03	2B1	152.51
B2	22.77	2B2	27.72
B3	209.62	2B3	198.34
B4	289.45	2B4	180.88
B5	249.17	2B5	124.67

B6	205.09	2B6	194.33
B7	320.73	2B7	246.02
B8	37.65	2B8	0
B9	24.67	2B9	0
B10	27.66	2B10	0
B11	19	2B11	0
B12	25	2B12	0

C1	412.13	2C1	0
C2	21.17	2C2	0
C3	254.65	2C3	0
C4	309.26	2C4	0
C5	269.6	2C5	0
C6	289.78	2C6	0
C7	332.61	2C7	0
C8	25.82	2C8	0
C9	20.27	2C9	0
C10	23.45	2C10	0
C11	19.82	2C11	0

C12	17.32	2C12	0
D1	271.63	2D1	0
D2	16.82	2D2	0
D3	236.35	2D3	0
D4	255	2D4	0
D5	234.17	2D5	0
D6	225.17	2D6	0
D7	264.82	2D7	0
D8	21.5	2D8	0
D9	21.83	2D9	0
D10	19.32	2D10	0
D11	21.81	2D11	0
D12	18.83	2D12	0

E1	261.63	2 E1	0
E2	31.69	2 E2	0
E3	264.5	2 E3	0
E4	244	2 E4	0
E5	222.5	2 E5	0

E6	264.67	2 E6	0
E7	299.67	2 E7	0
E8	23.51	2 E8	0
E9	27.49	2 E9	0
E10	12.16	2 E10	0
E11	25	2 E11	0
E12	21.29	2 E12	0